www.sciencemag.org/content/347/6223/779/suppl/DC1

Supplementary Materials for

A small-molecule inhibitor of the aberrant transcription factor CBFβ-SMMHC delays leukemia in mice

Anuradha Illendula, John A. Pulikkan, Hongliang Zong, Jolanta Grembecka, Liting Xue, Siddhartha Sen, Yunpeng Zhou, Adam Boulton, Aravinda Kuntimaddi, Yan Gao, Roger A. Rajewski, Monica L. Guzman, Lucio H. Castilla,* John H. Bushweller*

*Corresponding author. E-mail: jhb4v@virginia.edu (J.H.B.); lucio.castilla@umassmed.edu (L.H.C.)

Published 13 February 2015, *Science* **347**, 779 (2015)
DOI: 10.1126/science.aaa0314

This PDF file includes:

Materials and Methods

Synthetic Chemistry

Commercially obtained reagents were used as received. All reagents and anhydrous solvents used for Grignard reaction were freshly distilled. Progress of reactions was monitored by TLC performed on Analtech 250micron silica gel GF plates visualized with 254 nm UV light and also by mass spectrometry using a Waters single-quadrupole LCMS. All compounds were purified on Biotage Isolera Four Flash Chromatography system, using SNAP cartridges. All di-valent compounds were also purified by HPLC. Melting points were determined on a Mel-Temp manual melting point apparatus with a Fluke 51II thermocouple. ^{1}H and ^{13}C NMR spectra were recorded on a Bruker NMR spectrometer at 600MHz in CD3OD-d_4 + DCl and DMSO-d_6, with TMS as internal standard. Chemical shift values are reported in δ ppm units. Mass spectra were recorded on a Micromass AutoSpec Ultima Magnetic sector mass spectrometer in positive ESI mode.

General Procedure for the Synthesis of Substituted Benzimidazole Monomers

To a solution of appropriately substituted nitroaniline (1.0 mmol, 1 equiv) and aldehyde (1.0 mmol, 1 equiv) in ethanol (4mL), DMSO (0.4mL, 10%) sodium dithionite solution (3 mmol in 3mL water, 3 equiv) was added. The reaction mixture was heated at 80 ^{o}C and stirred for 5-8 hours. The reaction was followed by TLC until completion. The solvent was removed under reduced pressure, diluted with water, and neutralized with aqueous NH_4OH solution. The precipitate thus formed was filtered, washed with water, and dried under vacuum. The filtered product was purified by flash chromatography. The slowly solidifying solid was dissolved in a minimal amount of dichloromethane and triturated with hexanes by stirring overnight at r.t. The solid thus obtained was filtered and dried under vacuum to give the substituted benzimidazole.

AI-4-88

2-(pyridin-2-yl)-1*H*-benzo[*d*]imidazole (AI-4-88). The solid was collected to give a white powder; mp 223.0 – 224.1 °C (lit. 221 – 222 °C (*31*)); ^{1}H NMR (600 MHz, CD_3OD-d_4 + DCl): δ 7.61 – 7.62 (2H, dd, *J*=3.06 Hz), 7.70 – 7.72 (1H, dd, *J*=2.88 Hz, 8.34 Hz), 7.84 – 7.86 (2H, dd, *J*=3.12 Hz), 8.14 – 8.17 (1H, dd, *J*=1.56 Hz, 7.8 Hz), 8.39 – 8.40 (1H, d, *J*=7.92 Hz), 8.8754 – 8.8832 (1H, d, *J*=4.68 Hz).

AI-4-57

5-methoxy-2-(pyridin-2-yl)-1*H*-benzo[*d*]imidazole (AI-4-57). The solid was collected to give a white powder; mp 135.4 – 136.8 °C; ^{1}H NMR (600 MHz, CD_3OD-d_4 + DCl): δ 3.90 (3H, s), 7.1371 – 7.1557 (1H, dd, *J*=2.22 Hz, 8.94 Hz), 7.22 (1H, d, *J*= 1.92 Hz), 7.62 – 7.64 (1H, dd, *J*=1.92 Hz, 7.6 Hz), 7.65-7.66 (1H,

d, *J*=8.94 Hz), 8.07 – 8.10 (1H, dd, *J*= 1.38 Hz, 7.8 Hz), 8.25 – 8.26 (1H, d, *J*=7.92 Hz), 8.82 – 8.83 (1H, dd, *J*=4.68 Hz); ^{13}C NMR (600 MHz, CD_3OD-d_4 + DCl): δ 56.88, 97.07, 116.27, 118.99, 124.23, 127.23, 134.16, 139.63, 142.89, 148.09, 152.33, 161.14. HRMS: m/z $[M+H]^+$ calcd for $C_{13}H_{11}N_3O$; 226.0980; found: 226.0973.

AI-10-11

5-methoxy-2-(5-(2-methoxyethoxy)pyridin-2-yl)-1*H*-benzo[*d*]imidazole (AI-10-11). The solid was collected to give a white powder; mp 156.6 – 157.8 °C; ^{1}H NMR (600 MHz, CD_3OD-d_4 + DCl): δ 3.44 (3H, s), 3.81 – 3.82 (2H, t), 3.89 (3H, s), 4.32 – 4.33 (2H, t), 7.14 – 7.16 (1H, dd, *J*=2.28 Hz, 9.00 Hz), 7.22 – 7.23 (1H, d, *J*=2.16 Hz), 7.63 – 7.65 (1H, dd, *J*=2.76 Hz, 8.58 Hz), 7.65 – 7.66 (1H, d, *J*=8.94 Hz), 8.25 – 8.27 (1H, d, *J*=8.76 Hz), 8.50 (1H, d, *J*=2.7 Hz); ^{13}C NMR (600 MHz, CD_3OD-d_4 + DCl): δ 57.52, 60.00, 70.44, 72.47, 97.64, 116.52, 118.85, 123.07, 125.95, 127.71, 134.84, 135.39, 142.25, 148.94, 160.26, 161.57. HRMS: m/z $[M+H]^+$ calcd for $C_{16}H_{17}N_3O_3$; 300.1343; found: 300.1346.

AI-10-47

2-(pyridin-2-yl)-5-(trifluoromethoxy)-1*H*-benzo[*d*]imidazole (AI-10-47). The solid was collected to give a white powder; mp 104. – 105.9 °C; ^{1}H NMR (600 MHz, CD_3OD-d_4 + DCl): δ 7.63 – 7.64 (1H, dd, *J*=1.32 Hz, 8.88 Hz), 7.78 – 7.80 (1H, dd, *J*=3.00 Hz, 7.74 Hz), 7.86 (1H, s), 8.01 – 8.02 (1H, d, *J*=9.00 Hz), 8.21 – 8.24 (1H, dd, *J*=1.62 Hz, 9.42 Hz), 8.42 – 8.44 (1H, d, *J*=7.92 Hz), 8.95- 8.96 (1H, dd, *J*=4.68 Hz); ^{13}C NMR (600 MHz, CD_3OD-d_4 + DCl): δ 108.62, 117.25, 122.34, 129.44, 132.02, 133.65, 139.85, 142.77, 149.07, 151.33, 152.44. HRMS: m/z $[M+H]^+$ calcd for $C_{13}H_8F_3N_3O$; 280.0692; found: 280.0693.

Synthesis of dimers:

Method A
This method was used to synthesize AI-4-83 and AI-10-49 in three steps.

Step 1

Synthesis of di-bromo compounds. **5,5'-((oxybis(ethane-2,1-diyl))bis(oxy))bis(2-bromopyridine) (AI-10-43):** A mixture of 2-bromo-5-hydroxy pyridine (1.74 g, 10 mmol), diethylene glycol di(*p*-toluenesulfonate) (2.07 g, 5 mmol), and K_2CO_3 (6.85 g, 50 mmol) in dry DMF (30 mL) was heated at 90 ^{o}C for four hours. The cooled reaction mixture was poured over ice water. A precipitate was immediately formed which was filtered, washed with water, and dried under vacuum to give a pure white solid **AI-10-43** in (1.88 g, 90%); mp: 125.6 – 126.1 °C; ^{1}H NMR (600 MHz, $CDCl_3$): δ 3.90 – 3.92 (2H, t), 4.16 – 4.17 (2H, t), 7.10 – 7.12 (1H, dd, *J*=3.06 Hz, 8.64 Hz), 7.34 – 7.35 (1H, d, *J*=8.64 Hz),

8.06 – 8.07 (1H, d, *J*=3.00 Hz); ^{13}C NMR (600 MHz, $CDCl_3$): δ 68.42, 70.00, 125.32, 128.35, 132.69, 137.71, 154.86.

Step 2

Synthesis of dialdehyde. **5,5'-((oxybis(ethane-2,1-diyl))bis(oxy))dipicolinaldehyde (AI-10-44):** Under argon, the dibromo compound (**AI-10-43**, 2.1 g, 5 mmol x2) was dissolved in freshly distilled anhydrous THF (45 mL) in an oven dried two-neck roundbottom flask. The mixture was heated to 45 °C, *i*-PrMgCl•LiCl (10 mL, 1.3M in THF, 13 mmol) was added, followed by addition of dioxane (6.75 mL, 15%). The mixture was stirred at room temperature for 24 hours. Anhydrous DMF (1.45 mL, 20 mmol, 2 equiv) was added dropwise and stirred at room temperature for four hours. The reaction was monitored by TLC and quenched with a saturated NH_4Cl solution (5 mL). The THF layer was separated and diluted with ethyl acetate then extracted with a saturated NH_4Cl solution, water, and brine. The organic layer was collected and concentrated under reduced pressure to give a gummy solid. The solid was triturated with chilled methanol; the solid thus separated was filtered, and the crude filtrate was purified by column chromatography to give an off-white powder (0.5 g, 30%); mp: 146.2 – 147.4 °C; ^{1}H NMR (600 MHz, $CDCl_3$): δ 3.97 – 3.99 (2H, t), 4.28 – 4.30 (2H, t), 7.30 – 7.32 (1H, dd, *J*=2.7 Hz, 8.58 Hz), 7.92 – 7.94 (1H, d, *J*=8.64 Hz), 8.44 (1H, d, *J*=2.76 Hz), 9.97 (1H, s); ^{13}C NMR (600 MHz, $CDCl_3$): δ 68.32, 69.90, 120.92, 123.48, 138.98, 146.74, 158.34, 192.15.

Step 3

To a solution of appropriately substituted nitroaniline (2.0 mmol) and dialdehyde (1.0 mmol) in ethanol (8 mL) and DMSO (0.8 mL, 10%), a sodium dithionite solution (1.04 g, 6 mmol in 6 mL water) was added. The reaction mixture was heated at 80 ^{o}C and stirred for eight hours. The reaction was followed by TLC until completion. The solvent was removed under reduced pressure, diluted with water, and neutralized with aqueous NH_4OH solution. The precipitate thus formed was filtered, washed with water, and dried under vacuum. The filtered product was purified by flash chromatography. The slowly solidifying precipitate was dissolved in a minimal amount of dichloromethane and triturated with hexanes by stirring overnight at r.t. The solid thus obtained was filtered, and further purification was done by HPLC using acetonitrile and water as eluents. After evaporation of solvents, the solid was dried under vacuum to give substituted benzimidazole dimers.

AI-4-83

2,2'-(5,5'-((oxybis(ethane-2,1-diyl))bis(oxy))bis(pyridine-5,2-diyl))bis(6-methoxy-1*H*-benzo[*d*]imidazole) (AI-4-83). The solid was collected to give an off-white powder (0.17 g, 30%); mp 234.3 – 235.2 °C; ^{1}H NMR (600 MHz, CD_3OD-d_4 + DCl): δ 3.85 (3H, s), 3.96 – 3.97 (2H, t), 4.37 – 4.39 (2H, t), 7.00 –

7.02 (1H, dd, *J*=2.28 Hz, 8.94 Hz), 7.07 (1H, d, *J*=2.22 Hz), 7.54 – 7.55 (1H, d, *J*=9.00 Hz), 7.60 – 7.62 (1H, dd, *J*=2.76 Hz, 8.76 Hz), 8.14 – 8.15 (1H, d, *J*=8.76 Hz), 8.35 – 8.36 (1H, d, *J*=2.70 Hz); ^{13}C NMR (600 MHz, CD_3OD-d_4): δ 56.68, 69.85, 71.34, 96.93, 115.77, 118.09, 122.76, 125.24, 126.85, 133.77, 134.20, 141.88, 147.99, 159.72, 160.75. HRMS: m/z $[M+H]^+$ calcd for $C_{30}H_{28}N_6O_5$; 553.2199; found: 553.2203.

AI-10-49

2,2'-(5,5'-((oxybis(ethane-2,1-diyl))bis(oxy))bis(pyridine-5,2-diyl))bis(6-(trifluoromethoxy)-1*H*-benzo[*d*]imidazole) (AI-10-49). The solid was collected to give a white powder (0.3 g, 45%); mp 102 – 106 °C; ^{1}H NMR (600 MHz, CD_3OD-d_4 + DCl): δ 3.98 – 3.99 (2H, m), 4.41 – 4.42 (2H, m), 7.43 – 7.44 (1H, dd, *J*=1.5 Hz, 8.88 Hz), 7.67 (1H, d, *J*=1.26), 7.68 – 7.70 (1H, dd, *J*=2.58 Hz, 8.76 Hz), 7.83 – 7.84 (1H, d, *J*=8.94 Hz), 8.31 – 8.32 (1H, d, *J*=8.76 Hz), 8.47 (1H, d, *J*=2.46 Hz); ^{13}C NMR (600 MHz, CD_3OD-d_4 + DCl): δ 69.93, 71.13, 99.15, 108.34, 116.72, 121.14, 125.73, 132.74, 135.45, 135.23, 141.70, 148.38, 151.70, 159.90. HRMS: m/z $[M+Na]^+$ calcd for $C_{30}H_{22}F_6N_6O_5$; 683.1448; found: 683.1442.

Method B
This method was used to synthesize AI-4-71, AI-4-82, and AI-10-19 in two steps.

Step 1

General synthesis of dialdehyde compounds: A mixture of 5-hydroxypicolinaldehyde (Biogene Organics, 4 mmol), ethylene glycol di(*p*-toluenesulfonate) (2 mmol), and K_2CO_3 (2.6 g, 20 mmol) in dry DMF (10 mL) was heated at 90 ^{o}C for four hours. The cooled reaction mixture was poured over ice water. A precipitate was formed, which was filtered and washed with water then dried under vacuum to give a crude product. The crude product was purified by flash chromatography.

AI-12-24

5,5'-((oxybis(ethane-2,1-diyl))bis(oxy))dipicolinaldehyde. The solid was collected to give a white powder; mp 119.82-121.5 °C;^{1}H NMR (300 MHz, $CDCl_3$): δ 3.89 – 3.92 (2H, t), 4.25 – 4.28 (2H, t), 7.29 – 7.33 (1H, dd, *J*=2.79 Hz, 8.67 Hz), 7.92 – 7.95 (1H, d, *J*=8.64 Hz), 8.44 – 8.45 (1H, d, *J*=2.79 Hz), 9.97 (1H, s); ^{13}C NMR (600 MHz, $CDCl_3$): δ 68.36, 69.64, 71.13, 120.87, 123.47, 139.06, 146.62, 158.45, 192.15.

AI-12-73

5,5'-(3,6,9,12-tetraoxatetradecane-1,14-diylbis(oxy))dipicolinaldehyde. The solid was collected to give a white powder; mp 89-91.5 °C; ^{1}H NMR (300 MHz, $CDCl_3$): δ 3.64 – 3.72 (6H, m), 3.88 – 3.91 (2H, t), 4.24 – 4.28 (2H, t), 7.30 – 7.34 (1H, dd, *J*=2.79 Hz, 8.67 Hz), 7.92 – 7.95 (1H, d, *J*=8.67 Hz), 8.44 – 8.45 (1H, d, *J*=2.82 Hz), 9.97 (1H, s); ^{13}C NMR (600 MHz, $CDCl_3$): δ 68.41, 69.55, 70.76, 70.80, 71.12, 120.92, 123.49, 139.06, 146.55, 158.52, 192.14.

AI-12-38

5,5'-(propane-1,3-diylbis(oxy))dipicolinaldehyde (AI-12-38); mp: 148°C; ^{1}H NMR (300 MHz, $CDCl_3$): δ 2.37 – 2.45 (1H, m), 4.31 – 4.35 (2H, t), 7.30 – 7.34 (1H, dd, *J*=2.85 Hz, 8.7 Hz), 7.95 – 7.98 (1H, d, *J*=8.67 Hz), 8.44 – 8.45 (1H, d, *J*=2.76 Hz), 9.99 (1H, s); ^{13}C NMR (600 MHz, $CDCl_3$): δ 29.00, 64.92, 120.72, 123.55, 138.86, 146.74, 158.24, 192.12.

Step 2 (see Method A, Step 3)

AI-10-19

1,3-bis((6-(6-methoxy-1*H*-benzo[*d*]imidazol-2-yl)pyridin-3-yl)oxy)propane (AI-10-19). The solid was collected to give an off-white powder; mp 239.9 – 240.8 °C; ^{1}H NMR (600 MHz, DMSO-d_6 + DCl): δ 2.31 – 2.35 (1H, m), 3.87 (3H, s), 4.43 – 4.45 (2H, t), 7.16 – 7.17 (1H, dd, *J*= *J*=2.34 Hz, 8.94 Hz), 7.19 (1H, d, *J*=2.1 Hz), 7.68 – 7.69 (1H, d, *J*=8.88 Hz), 7.83 – 7.85 (1H, dd, *J*=2.76 Hz, 8.88 Hz), 8.58 – 8.59 (1H, d, *J*=2.76 Hz), 8.72 – 8.74 (1H, d, *J*=8.82 Hz); ^{13}C NMR (600 MHz, DMSO-d_6 + DCl): δ 28.44, 55.39, 64.99, 94.51, 101.27, 111.44, 112.03, 112.48, 119.47, 121.89, 122.19, 129.42,135.60, 137.30, 137.47, 138.40, 141.48, 149.99, 155.28, 155.42, 156.17. HRMS: m/z $[M+H]^+$ calcd for $C_{29}H_{26}N_6O_4$; 523.2088; found: 523.2083.

AI-4-82

1,2-bis(2-((6-(6-methoxy-1*H*-benzo[*d*]imidazol-2-yl)pyridin-3-yl)oxy)ethoxy)ethane (AI-4-82). The solid was collected to give a light tan powder; mp 105.2 – 107.4 °C; ^{1}H NMR (600 MHz, CD_3OD-d_4 + DCl): δ 3.77 (2H, s), 3.84 (3H, s), 3.92 (2H, m), 4.30 (2H, m), 7.04 – 7.05 (1H, d, *J*=8.94 Hz), 7.10 (1H, d, *J*=1.68 Hz), 7.56 – 7.57 (1H, d, *J*=8.94 Hz), 7.59 – 7.61 (1H, d, *J*=7.38 Hz), 8.15 – 8.16 (1H, d, *J*=8.58 Hz), 8.40 (1H, s); ^{13}C NMR (600 MHz, CD_3OD-d_4 + DCl): δ 56.77, 70.11, 70.60, 72.08, 96.93, 115.84, 118.09, 122.64, 125.46, 126.76, 133.69, 134.24, 141.61, 147.81, 159.50, 160.66. HRMS: m/z $[M+H]^+$ calcd for $C_{32}H_{32}N_6O_6$; 597.2462; found: 597.2455.

AI-4-71

1,14-bis((6-(6-methoxy-1*H*-benzo[*d*]imidazol-2-yl)pyridin-3-yl)oxy)-3,6,9,12-tetraoxatetradecane (AI-4-71). The solid was collected to give a white powder; mp 183°C (dec); ^{1}H NMR (600 MHz, CD_3OD-d_4 + DCl): δ 3.66 (2H, s), 3.68 – 3.69 (2H, m), 3.72 – 3.73 (2H, m), 3.87 (3H, s), 3.91 – 3.92 (2H, t), 4.30 – 4.31 (2H, t), 7.11 – 7.13 (1H, dd, *J*=2.22 Hz, 8.94 Hz), 7.14 – 7.15 (1H, d, *J*=2.04 Hz), 7.60 – 7.62 (2H, d, *J*=8.94 Hz), 8.17 – 8.19 (1H, d, *J*=8.7 Hz), 8.46 – 8.47 (1H, d, *J*=2.52 Hz); ^{13}C NMR (600 MHz, CD_3OD-d_4 + DCl): δ 56.81, 70.09, 70.60, 71.78, 71.83, 72.00, 96.93, 115.88, 118.17, 122.50, 125.51, 126.76, 133.69, 134.30, 141.54, 147.79, 159.37, 160.66. HRMS: m/z $[M+Na]^+$ calcd for $C_{36}H_{40}N_6O_8$; 707.2800; found: 707.2797.

FRET assays.

Cerulean-Runt domain was expressed and purified as described previously (*13*). Venus-CBFβ-SMMHC was constructed by inserting 6xHis tag and Venus into pET22b vector between NdeI and NcoI sites, and by inserting CBFβ-SMMHC (the CBFβ-SMMHC construct contains 369 amino acids, 1-166 from CBFβ and 166-369 from MYH11 (amino acids 1526-1730)) between the NcoI and BamHI sites. The fusion protein was purified by standard Ni-affinity chromatography with an on column benzonase treatment to remove residual DNA contaminants. Proteins were dialyzed into FRET buffer (25mM Tris-HCl, pH 7.5, 150mM KCl, 2mM $MgCl_2$) prior to use. Protein concentrations were determined by UV absorbance of the Cerulean and Venus at 433 and 513 nm, respectively. Cerulean-Runt domain and Venus-CBFβ-SMMHC were mixed 1:1 to achieve a final concentration of 10 nM in 96 well black COSTAR (Corning Life Sciences, Lowell, MA, USA) plates. DMSO solutions of compounds were added to a final DMSO concentration of 5% (v/v) and the plates incubated at room temperature for one hour in the dark. A PHERAstar microplate reader (BMG Labtech, Durham, NC, USA) was used to measure fluorescence (excitation at 433 nm and emission measured at 474 and 525 nm). For IC_{50} determinations, the ratios of the fluorescence intensities at 525 nm and 474 nm were plotted versus the log of compound concentration, and the resulting curve was fit to a sigmoidal curve using Origin7.0 (MicroCal, Northampton, MA, USA). Three independent measurements were performed and their average and deviation were used for IC_{50} data fitting.

Protein NMR spectroscopy

All NMR experiments were performed at 30 °C on a Bruker 800 MHz instrument equipped with a cryogenic probe. All NMR samples were prepared in 50 mM potassium phosphate, 0.1 mM EDTA, 0.1 mM NaN_3, 1 mM DTT, and 5% (v/v) D_2O at a final pH of 7.5. ^{15}N-^{1}H HSQC experiments utilized a 500 μM sample and ^{13}C-^{1}H HSQC experiments were conducted on a 1 mM sample. All NMR data was processed using NMRPipe and Sparky. Weighted chemical shift changes in parts per million were calculated by using the equation: $\Delta(^{15}N + {}^{1}HN) = |\Delta\delta HN|+(|\Delta\delta N|/4.69)$.

Isothermal titration calorimetry

The 369 amino acid CBFß-SMMHC construct consisting of CBFß residues 1-166 and 166-369 from MYH11 (MYH11 amino acids 1526-1730) was cloned into a modified pET22b vector with an N-terminal 6xHis tag and a Tev protease site and was expressed in Rosetta2(DE3) cells (Novagen) in Terrific Broth media with 1mM IPTG induction for 8 hours at 30°C. CBFß-SMMHC was purified via Ni-affinity chromatography followed by benzonase treatment and Tev protease digestion overnight. The fusion protein was then passaged a second time through the Ni-NTA column followed by Q-Sepharose ion exchange chromatography to remove residual nucleic acid. Additional purification was achieved via size exclusion chromatography using a Sephacryl S300 column.

Purified CBFß-SMMHC was dialyzed into 1 L of ITC buffer (12.5 mM KPi (pH 6.5), 150 mM NaCl, 2 mM $MgCl_2$, 1 mg/mL NaN_3, 1 mM DTT, and 0.25% DMSO) for 4 hours. AI-10-49 was added separately to 10 mL of ITC buffer to a final concentration of 2 μM. The concentration of AI-10-49 was verified using ^{1}H NMR on a Bruker 600 MHz NMR spectrometer using DSS as a standard. All ITC measurements were carried out at 30 °C on a MicroCalorimetry System (MicroCal, Inc.). CBFß-SMMHC and AI-10-49 samples were degassed for 20 min and 8 μL injections of 2μM AI-10-49 were made to a 400 nM solution of CBFß-SMMHC in the calorimetric cell.

A biphasic transition was consistently observed in the ITC data indicative of more than one process contributing to the observed heats. As a result of this and because of the relatively small heats observed, this data could not be analyzed using the standard software available on the calorimeter which uses the heat values to determine a K_D. Rather, data were analyzed utilizing Origin 7.5 (Origin Lab) and were fit to a one-site sigmoidal binding curve after correction for dilution enthalpy to derive apparent K_D values. The measurement was repeated three times and values are reported as the average ± standard deviation.

Cell culture assays in cell lines

ME-1 cells (DSMZ, Germany) were cultured in RPMI 1640 with 20 % fetal bovine serum, and 25 mM HEPES. U937 and Kasumi-1 (both from ATCC, USA) cells were cultured in RPMI 1640 with 10 % fetal bovine serum. The linker length assays: $5x10^5$ ME-1, U937 and Kasumi-1 cells were cultured for 24 hours in DMSO, or different concentrations (0.6, 1.25, 2.5, 5, and 10 μM) of AI-4-83, AI-4-82, AI-4-71, or AI-10-19); each in triplicate, using 96 well plates. Cell viability was estimated using the MTT kit, CellTiter 96® AQ_{ueous} One Solution (Promega, PA). The experiments were replicated at least twice.

HL-60 (purchased 9/2010, ATCC), KG-1 (purchased 9/2010, ATCC), THP-1 (purchased 9/2010, ATCC), Kasumi-1 (purchased 4/2011, ATCC), TUR

(purchased 1/2010, ATCC), U937 (purchased 12/2009, ATCC), and MOLM-13 (kind gift form G. Chiosis-MSKCC 7/2010, 2/2014 authenticated; biosynthesis) cell lines were cultured in Iscove's Modified Dulbecco's Medium (IMDM; Life technologies) supplemented with 10%~20% fetal bovine serum (FBS) according to culture conditions indicated by ATCC and 1% penicillin/streptomycin (Pen/Strep; Life Technologies). All cell lines were tested for mycoplasma. Cells were cultured at 300,000 cells per ml in 96 well plates for 24 and 48 hours in DMSO, or different of AI-10-47, AI-410-49, AI-4-57, or AI-4-88); each in duplicate or triplicate. Cell viability was evaluated using DAPI by flow cytometry. Data was analyzed using FlowJo software and Graphpad Prism software.

Co-immunoprecipitation Analysis

ME-1 cells were treated for 3 and 6 hours with DMSO or 1μM AI-10-49, and whole cell lysates were prepared by lysing the cells in RIPA lysis buffer for western blot analysis. Protein samples were resolved in 10% polyacrylamide gel. Antibodies used include RUNX1 antibody (cat#39000, Active Motif), CBFβ antibody (generously provided by Dr. Nancy Speck, University of Pennsylvania School of Medicine, Philadelphia PA; ref. (*32*), and GAPDH (cat#3683, Cell Signaling Technology).

For co-immunoprecipitation assays, $3x10^6$ ME1 cells were treated with AI-10-49 (1 μM) for various time points. Cells were lysed in modified RIPA buffer (50 mM Tris pH7.5, 150 mM NaCl, 1 % NP40, 0.25 % sodium deoxycholate and 1 mM EDTA). RUNX1 was immunoprecipitated from cell lysates using anti-RUNX1 antibody (cat#39000, Active Motif) and protein-A Agarose beads (Roche Applied Science) according to manufacturer's instructions. Briefly, cell lysates were mixed with protein A agarose beads and 2 μg antibody in IP buffer I (50 mM Tris pH7.5, 150 mM NaCl, 0.5 % NP40, 0.25 % sodium deoxycholate) and rotated at 10 rpm for five hours. Agarose beads were washed twice with IP Buffer I followed by washing with IP buffer II (50mM Tris pH 7.5, 0.1 % NP40, 0.05 % sodium deoxycholate). All lysis, immunoprecipitation, and washing steps for treatment samples included 1 μM AI-10-49. The beads were heated at 95˚C for 12 minutes in Western blot loading buffer (100 mM Tris-HCL pH6.8, 200 mM DTT, 4% SDS, 0.2% Bromophenol-blue, 20% glycerol). The eluted protein was resolved in a 10% polyacrylamide gel. CBFβ and CBFβ-MYH11 were detected using anti-CBFβ antibody (*32*). The membrane was re-probed with anti-RUNX1 antibody and detected using Clean-*Blot IP Detection Reagents* (Thermo Scientific). Relative band intensities were quantified using ImageJ software.

Quantitative RT-PCR analysis

ME1 and U937 cells were treated with DMSO or AI-10-49 (1μM) for 6 and 12 hours. After RNA extraction with Trizol (Invitrogen), first-strand cDNA was generated using 200 U Super-Script III reverse transcriptase (Invitrogen) and 0.5 μg oligo dT primer. The quantitative PCR was performed using SYBR Green PCR master mix (Applied Biosystems) containing 0.25 μM gene-specific primers

and detected in ABI PRISM 7000 sequence detection system (Applied Biosystems) according to the manufacturer's instructions using the following primers: *RUNX3F* (5'-CAGAAGCTGGAGGACCAGAC-3), *RUNX3R (5'-*GTCGGAGAATGGGTTCAGTT-3'), *CSF1RF (*5'-ATTGTCAAGGGCAATGCCCGCC-3'), *CSF1R (*5'-ATTGGTATAGTCCCGCTCTCTCC-3'), *CEBPAF* (5'-AAGGTGCTGGAGCTGACCAG-3'), *CEBPAR* (5'-AATCTCCTAGTCCTGGCTCG-3'), *PIN1F* (AAGATGGCGGACGAGGAG-3'), *PIN1R* (5'-CACTCAGTGCGGAGGATGAT-3'), *ACTNBF (*5'-AGAAAATCTGGCACCACACC-3') and *ACTNBR (*5'-AGAGGCGTACAGGGATAGCA-3'). Relative expression levels were normalized to that of *ACTNB* expression.

Chromatin Immunoprecipitation Assays

Three million ME1 cells were treated with DMSO or AI-10-49 (1 μM) for six hours. Cross-linking of proteins to DNA was accomplished by the addition of 1 % formaldehyde for 10 minutes to cultured cells at 37 °C. After sonication, the chromatin was immunoprecipitated with 5 μg of anti-RUNX1 antibody (cat#39000, Active Motif) or anti–immunoglobulin G (clone#E1512, Santa Cruz Biotechnology) at 4 °C overnight. Antibody bound complexes were isolated with protein A agarose beads (Roche Applied Science) for three hours at 4 ºC, and washed with various buffers: once with Low Salt Immune Complex Wash Buffer (0.1 % SDS, 1 % Triton X-100, 2 mM EDTA, 20 mM Tris-HCl pH 8.1, 150 mM NaCl), once with High Salt Immune Complex Wash Buffer (0.1 % SDS, 1% Triton X-100, 2 mM EDTA, 20 mM Tris-HCl pH 8,1, 500 mM NaCl), once with LiCl Immune Complex Wash Buffer (0,25 M LiCl, 1 % IGEPAL-CA630, 1 % sodium deoxycholate, 1mM EDTA, 10 mM Tris pH 8.1) and twice with TE-buffer (10 mM Tris-HCl, 1 mM EDTA pH 8.0). Antigen/antibody complexes were extracted with 500 μl of elution buffer (1 % SDS and 0.1 M $NaHCO_3$, eluted from the beads, treated overnight with 5 M NaCl at 65 ºC, and DNA was purified using phenol-chloroform isoamyl-alcohol method. The presence of *RUNX3, CSF1R, ACTB,* and *PIN1* promoter regions was quantified by RT-PCR with the following primers: *RUNX3 oligo#1: RUNX3pF (*5'-TGAGCTGAGGTTGGGTTGA-3') and *RUNX3pR (*5'-AGGCTCTGGTGGGTACGA-3'); *RUNX3* oligo#2: *RUNX3pF* (5'-TCCCTGGAAATTGAGCACCT-3') and *RUNX3pR* (5'-GGGAAGCAGAAAGGACAAGG-3'); *CSF1R* oligo#1: *CSF1RpF* (5'-TTTAGAAGGGCCCCAAACTT-3') and *CSF1RpR* (5'-TCTGCACTGGCTGTTTGTCT-3'), *CSF1R* oligo#2: *CSF1RpF* (5'-AGTGTGACTCCTCCAAGATTGT-3') and *CSF1RpR* (5'-AAGACAGCGGTACTCTCAAAG-3'); *CEBPA* oligo#1: *CEBPApF* (5'-TGCAGCCTCGGGATACTCCT-3') and *CEBPApR* (5'-AGAGCCGCGGCGCTCGCTCCAA-3'); *CEBPA oligo#2: CEBPApF* (5'-CCCTCCAAAACCACAAAGCA-3') and *CEBPApR* (5'-GCGGGCAGGGTAGATTAGAA-3'); *ACTBpF* (5'-CTTCTACAATGAGCTGCGTGTGG-3'), *ACTBpR* (5'-ATGGCTGGGGTGTTGAAGGTCTCA-3'), *PIN1pF* (5'-

GGCATTAGCCAATCCATAAGC-3") and *PIN1pR* (5'-GGCCTTCTATTGGGTAGAAG-3'). The levels of enrichment were normalized to that obtained with a control IgG antibody and calculated as the fold increase above that measured for the DMSO sample. The occupancy of RUNX1 on target DNA regions was estimated as "fold enrichment to IgG" using the 2e-ΔΔCt method. The occupancy of RUNX1 was also estimated as "fold enrichment to DMSO" by calculating the fold enrichment to IgG and normalizing to the value of the DMSO treated sample.

Compound Formulation

All dosing solutions were formulated in-house and sterile filtered through 0.22-micron sterile filters prior to use. All solutions were stable over two weeks at 25°C as assessed by HPLC.

AI-4-57

A maximum solubility of approximately 54 mg/mL in 0.1 M Captisol (Ligand Pharmaceuticals, La Jolla, CA, USA) was achieved with the hydrochloride salt of AI-4-57. A dosing solution of 27.9 mg/mL in 0.1 Captisol was prepared.

AI-10-49

A maximum solubility of approximately 100 mg/mL in DMSO was achieved. A dosing solution of 83 mg/mL in DMSO was prepared.

Pharmacokinetic Studies

The University of Kansas Institutional Animal Care and Use Committee approved this study and appropriate guidelines for the use of animals were observed during all aspects of the study. Prior to the study, mice were fasted at least three hours and water was available *ad libitum*. Animals were housed on a 12-hour light/dark cycle at 72-74°C and 30-50% relative humidity.

For intraperitoneal dosing 24 – 28 gm male C57BL/6 mice (Harlan Laboratories, USA) were manually restrained and injected in the peritoneal cavity midway between the sternum and pubis and slightly off the midline of the mouse. A 1-cc syringe with a 27-gauge needle was used for each injection. Blood was collected from the animals according to scheduled time points. Animals were anesthetized with isoflurane and blood drawn via cardiac puncture. Blood was immediately transferred to 1.5 mL heparinized microcentrifuge tubes and centrifuged at 4000 rpm for ten minutes. Plasma was then transferred to clean tubes and frozen. Due to exsanguination, the animals did not wake from the anesthesia and death was insured while under anesthesia by thoracotomy. This method is consistent with the recommendations of the AVMA Guidelines on Euthanasia for use of exsanguination as a means of euthanasia.

Noncompartmental pharmacokinetic analysis of the test compound plasma concentration-time data was conducted using PK Solutions 2.0 (Summit Research Services, Montrose, CO, USA).

Bioanalysis

Materials – Methyl-*t*-butyl ether (MtBE) and HPLC grade acetonitrile (ACN) were obtained from Fisher (NJ, USA). Trifluoroacetic acid (TFA) and formic acids was from Fluka (St. Louis, MO, USA). Dimethylsulfoxide (DMSO) was obtained from Sigma (St. Louis, MO, USA) and was Hybri-Max grade.

General Equipment - A VX-2500 multi-tube vortexer from VWR (West Chester, PA, USA) and an accuSpin Micro 17 centrifuge from Fisher (NJ, USA) were used in the sample preparation. Solvent evaporation was carried out on a CentriVap concentrator from Labconco (Kansas City, MO, USA) with a Büchi V-800 vacuum controller (Switzerland).

AI-4-57 - An LC/MS/MS method was developed for AI-4-57 using 2-(2-pyridyl) benzimidazole (Aldrich, St. Louis, MO, USA) as an internal standard. Samples were analyzed on an Applied Biosystems 3200 QTRAP (Grand Island, NY, USA) operated in positive ion mode with a Shimadzu SCL-10A vp controller, SIL-20AC autosampler, LC-20AD pumps and CTO-20A column oven (Kyoto, Japan). LC/MS chromatography conditions included a Zorbax SB C18, 5 µm, 2.1 x 150 mm at 40 °C with a mobile phase flow rate of 0.25 mL/min. The gradient elution consisted of solvents A and B with A) 5/95/0.1, and B) 95/5/0.1: acetonitrile/water/formic acid, respectively. The gradient consisted of 95% B in four minutes, 95% B for 0.5 minutes, 95 – 1% B in 0.5 minutes, and 1% B for three minutes. Samples were held at 15 °C and 10 µL was injected. The retention time of AI-4-57 is 3.2 minutes. 2-(2-pyridyl) benzimidazole (IS) elutes at 2.9 minutes.

Mass spectrometry conditions consisted of a curtain gas of 10 xx, a temperature of 600 °C, GS1 & GS2 of 30 xx, and an IS voltage of 5500 xx. Monitored AI-4-57 transitions were 226.2/211.1, DP = 75, EP = 5.5, CEP = 12, CE = 30, CXP = 4. Monitored IS transitions were 196.1/92.1, DP = 90, EP = 5.5, CEP = 12, CE = 37, CXP = 2. Two sets of standards and samples, a high concentration and a low concentration range were run. Following the addition of 10 ⌠L of internal standard, the standards prepared in plasma and samples were charged with acetonitrile, vortexed, centrifuged and the supernatant transferred to clean tubes, which were then dried under vacuum. The standards and samples were reconstituted in 50/50 acetonitrile/water, vortexed, centrifuged, and the supernatant transferred to autosampler vials for analysis. The validation sets consisted of blank plasma, a standard curve with the range of 1, 5, 10, 50 100, 500 and 1000 ng/mL AI-4-57 (R^2 > 0.9994) and six quality control samples each at the level of 5 ng/mL (low QC), 50 ng/mL (mid QC) and 500 ng/mL (high QC).

AI-10-49 – HPLC analysis was performed with an LC system consisting of a Shimadzu SCL-10Avp controller, SIL-10A autosampler, LC-10ADvp pumps, SPD-10Avp detector and CTO-10Avp column oven. Data acquisition, peak integration and calculation were accomplished with LabSolutions software. A 4.6

x 150 mm Atlantis T3 5 micron column was used for fractionation using a gradient mobile phase consisting of solvents A and B with ratios of 5/95/0.1 and 95/5/0.1 acetonitrile/water/TFAacid, respectively, at 50 -95% B in four minutes, 95% B for 2 min, 95 – 50% B in 0.5 min, and 50% B for 4.5 min. Flow rate was 1 mL/min at 45°C. The injection volume was 40 microliters with detection at 325 nm. Quantiation was versus external standards prepared in blank plasma over a linear range of 25 – 750 ng/mL (R^2 > 0.995)

Extraction of plasma samples was conducted on 100 µL of the respective samples using 0.5 mL of MtBE after adding 10 µL of AI-10-49 spiking solution (10X), vortexing, and allowing the sample sit at room temperature for 5 min. The two phase mixture was vortexed for five min then centrifuged at 12,000 rpm for five min. 450 µL of the MtBE layer was transferred to clean tubes and evaporated to dryness. The resulting residue was reconstituted in 100 µL of 50/50/0.1, ACN/H2O/TFA and vortexed followed by centrifugation at 12,000 rpm for five min. 90 µL of the supernatant was transferred to autosampler vials with polypropylene inserts and analyzed.

Toxicology Studies

The cumulative toxicity of AI-10-49 was evaluated after daily administration for seven days. These studies did not include maximum tolerated dose or long term (> 30 days) toxicity. Six week old C57BL/6 female mice were treated with daily intraperitoneal injection of DMSO or 200mg/kg AI-10-49 for seven days (n=3 to 4 per group). The appearance of mice was analyzed for signs of toxicity, including grooming, motility, and weight. Four hours after last injection, peripheral blood cells were analyzed by flow cytometry and quantified with hemocytometer. Mice were then euthanized for tissue harvesting. Bone marrow hematopoietic progenitors were analyzed by flow cytometry, including hematopoietic stem and multilineage progenitors [LSK+= Lin(-), kit(+), Sca1(+)], common myeloid progenitors [CMP=Lin(-)Sca1(-)kit(+)CD34(+)CD16/32(-)], granulocyte/monocyte progenitor [GMP=Lin(-)Sca1(-)kit(+)CD34(+)CD16/32(+)], and megakaryocyte/erythroid progenitors [MEP=Lin(-)Sca1(-)kit(+)CD34(-)CD16/32(-)]. Parafin-sections of bone marrow, liver, lung, spleen, intestine, and brain were prepared and stained with hematoxylin & eosin for the analysis of tissue architecture. Slides were analyzed using an Olympus BX41 microscope, with Olympus 4x and 10x lenses, Evolution MP5.0 color camera (Media Cybernetics, Canada), and QCapturePro software. Antibodies included Gr-1 (clone#RB6-8C5), Mac1 (clone#M1/70), B220 (clone#RA3-6B2), CD3 (clone#17A2 and clone#145-2C11), Ter119 (clone#Ter119), c-kit (clone#2B8), Sca-1 (clone#D7), CD34 (clone#RAM34), all from BD Biosciences. In addition, CD16/32 (clone#93, eBioscience) was also used.

Leukemia transplantation studies in mice

The experiments with animals were performed in accordance with a protocol

reviewed and approved by the University of Massachusetts Institutional Animal Care and Use Committee. Leukemic cells carrying *Cbfb*$^{+/MYH11}$ and *Nras*$^{+/G12D}$ oncogenic alleles were generated in CD45.2 C57BL/6 mice, as previously described (*26*). Briefly, 2x10^3 *Cbfb*$^{+/MYH11}$;*Nras*$^{+/G12D}$ leukemic cells were transplanted into each of 22 sublethally irradiated six to eight week old CD45.1 C57BL/6 female mice. The number of mice per group was selected in preliminary assays to achieve statistical power under the established experimental conditions. At day five post-transplantation, mice were randomized into two groups, and injected intraperitoneally for ten days with 50 µL DMSO or AI-10-49 (200 mg/kg) in DMSO. Mice were kept under observation by more than one person to determine the median leukemia latency, and were euthanized once signs of disease were detected, including reduced motility and grooming activity, hunched back, pale paws (anemia), and hypothermia. At time of euthanasia, peripheral blood and spleen cell were extracted and analyzed as previously described (*9*). Leukemia burden was analyzed in peripheral blood by measuring the total white blood cell counts and the number of cells in the c-kit(+)-gated population.

Statistical Methods for Leukemia transplantation studies in mice

The analysis of leukemia latency and P value were estimated using Survival package in R software(*33*). Median latency for DMSO group=33.5 days (95% confidence interval (33, NA)). Median latency AI-10-49 treated group= 61 days (95% confidence interval (47, NA)). P-value between groups = 2.71e-06; using log-rank test.

Analysis of inv(16) samples

Primary AML and cord blood samples

Cryopreserved primary AML samples were obtained with informed consent and Weill Cornell Medical College institutional review board approval, from the University of Pennsylvania Stem Cell & Xenograft Core Facility, or from Erasmus University Medical Center (generously provided by Ruud Delwel). Umbilical cord blood (CB) was obtained from the New York Blood Center (NYBC). AML samples were thawed and cultured as described previously (*34*). Briefly, AML samples with cell viability below 50% at thawing were excluded from the study. Cells were cultured in Iscove's Modified Dubecco's Medium (IMDM) supplemented with 10% FBS, 16.7 µg/mL low-density lipoprotein (EMD Millipore), β-mercaptoethanol, L-glutamine, penicillin, streptomycin, and supplemented with 20 ng/ml FLT-3 ligand, 50 ng/ml SCF, 20 ng/ml IL-3 and 20 ng/ml IL-6. CD34(+) AML or CD34(+) cord blood cells were isolated using antibody-coupled magnetic bead separation from Milteneyi Biotech (*35*), and cultured for one hour before treatment with AI-10-47 and AI-10-49.

Flow Cytometry

Apoptosis assays were performed as described previously(*35*). Briefly, 48 hours post-treatment, primary AML cells were stained for the surface antibodies CD45-APCH7 (clone 2D1), CD38-V450 (clone HB7), and CD34-PECy7 (clone 581) (all from BD Biosciences) for 30 min prior staining in 200 µL of Annexin V buffer (0.01 mol/L HEPES/NaOH, 0.14 mol/L NaCl, 2.5 mmol/L $CaCl_2$) containing Annexin V fluorescein (BD Biosciences) and 7-aminoactinomycin D (Molecular Probes-Life Technologies). Viability was determined as the percent of Annexin V negative/7-AAD negative cells. Percent viability was represented relative to the DMSO control. For differentiation assays primary AML samples were stained with CD64-FITC (clone 10.1), CD14-APC-Cy7 (clone MoP9), CD38-APC (clone HB7), CD11b-Alexa-Fluor700 (clone CRF44), CD10-PE (clone HI10a), CD34-PECy7 (clone 581), and CD45-V500 (clone 2D1) (all from BD Biosciences) for 30 min prior staining with Annexin V and 7-AAD. Tubes were incubated at room temperature for 15 min and then analyzed with a BD LSRII flow cytometer. Analysis was performed using FlowJo Software (TreeStar data analysis software).

Colony-forming assays
After treatment for 48 hours cells were plated in MethoCult medium with recombinant human (rh) SCF, rh GM-CSF, rh IL-3, rh EPO (H4434; StemCell Technologies) as previously described (*35*). The colony-forming units (CFUs) in treated cells were normalized to DMSO control.

Quantitative RT-PCR.
Primary AML cells with inv(16) were treated with AI-10-49 for 6 to 48 h, and subjected to RNA extraction using RNeasy Plus Mini Kit (Qiagen). Quantitative RT-PCR for *CBFB-MYH11* was performed using a Taqman® probe for *CBFB-MYH11* (Hs03043618) and TaqMan® RNA-to-CT™ 1-Step Kit (Life Technologies). Taqman® probe for GAPDH (Hs02758991) was used a housekeeping control.

Fig. S1

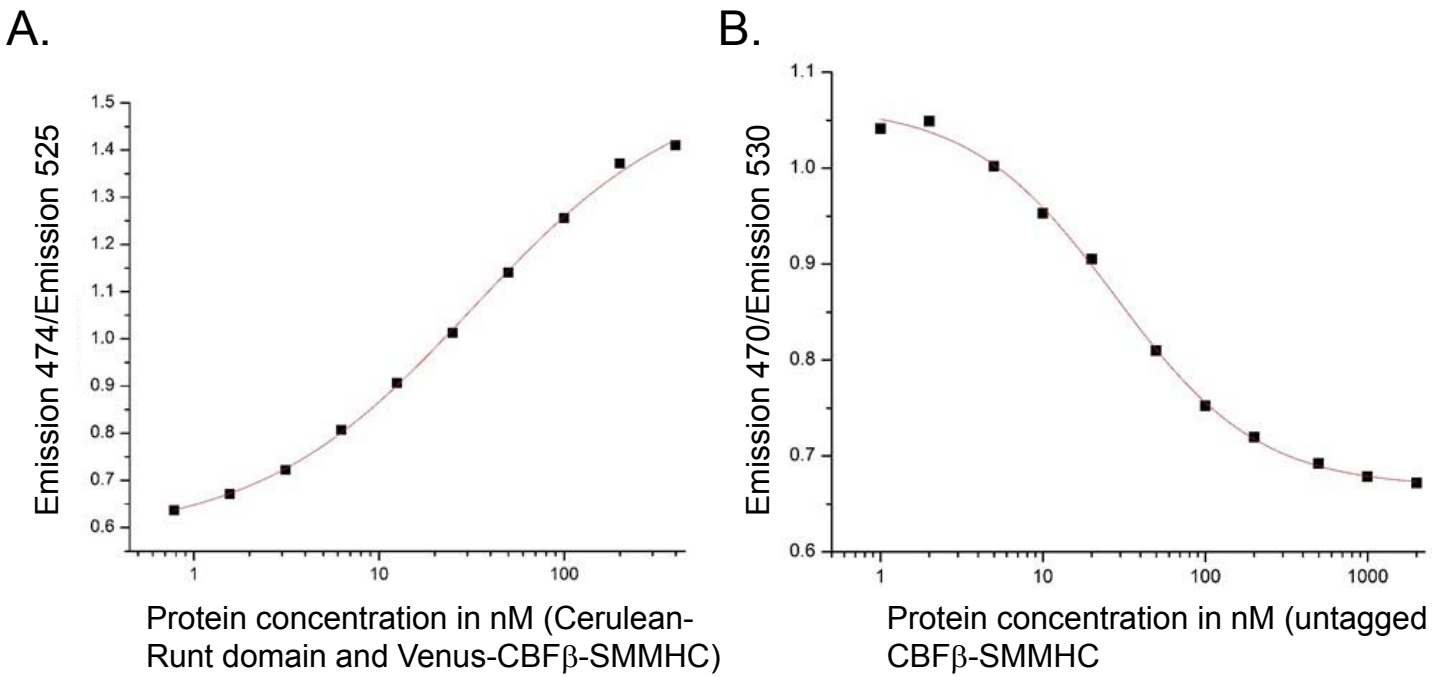
A.
Emission 474/Emission 525
1.5
1.4
1.3
1.2
1.1
1.0
0.9
0.8
0.7
0.6
1
10
100
Protein concentration in nM (Cerulean-Runt domain and Venus-CBFβ-SMMHC)
B.
Emission 470/Emission 530
1.1
1.0
0.9
0.8
0.7
0.6
1
10
100
1000
Protein concentration in nM (untagged CBFβ-SMMHC

Fig. S1

A. Results of a K_d determination by serial dilution for binding of Cerulean-Runt domain to Venus-CBFβ-SMMHC. Fitting of the data yielded a K_d of 16 nM, in good agreement with the value of 8 nM we have determined previously using isothermal titration calorimetry for binding of untagged CBFβ-SMMHC to the Runt domain (*8*). B. Results of a competition experiment carried out with the concentration of Cerulean-Runt domain and Venus-CBFβ-SMMHC held at 16 nM and addition of untagged CBFβ-SMMHC to compete the tagged protein off Cerulean-Runt domain. Fitting using the Cheng-Prusoff equation yields a K_i of 14 nM, in good agreement with the measured K_d, and validating that we can measure dissociation of Cerulean-Runt domain from Venus-CBFβ-SMMHC by inhibitors using this assay.

Fig. S2

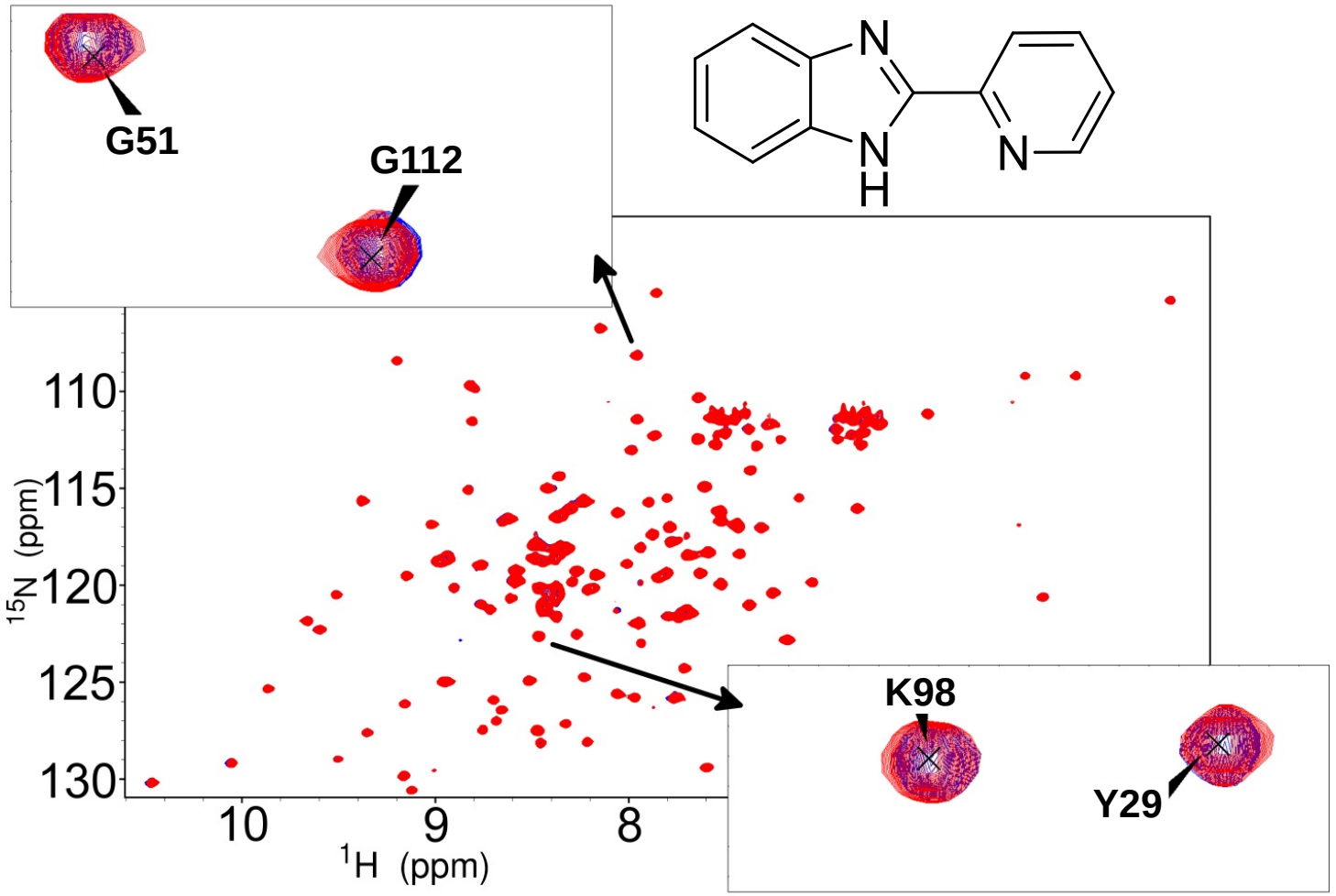

Fig. S2

^{15}N-^{1}H HSQC spectrum of CBFβ alone (blue) and CBFβ + AI-4-88 (red).

Fig. S3A

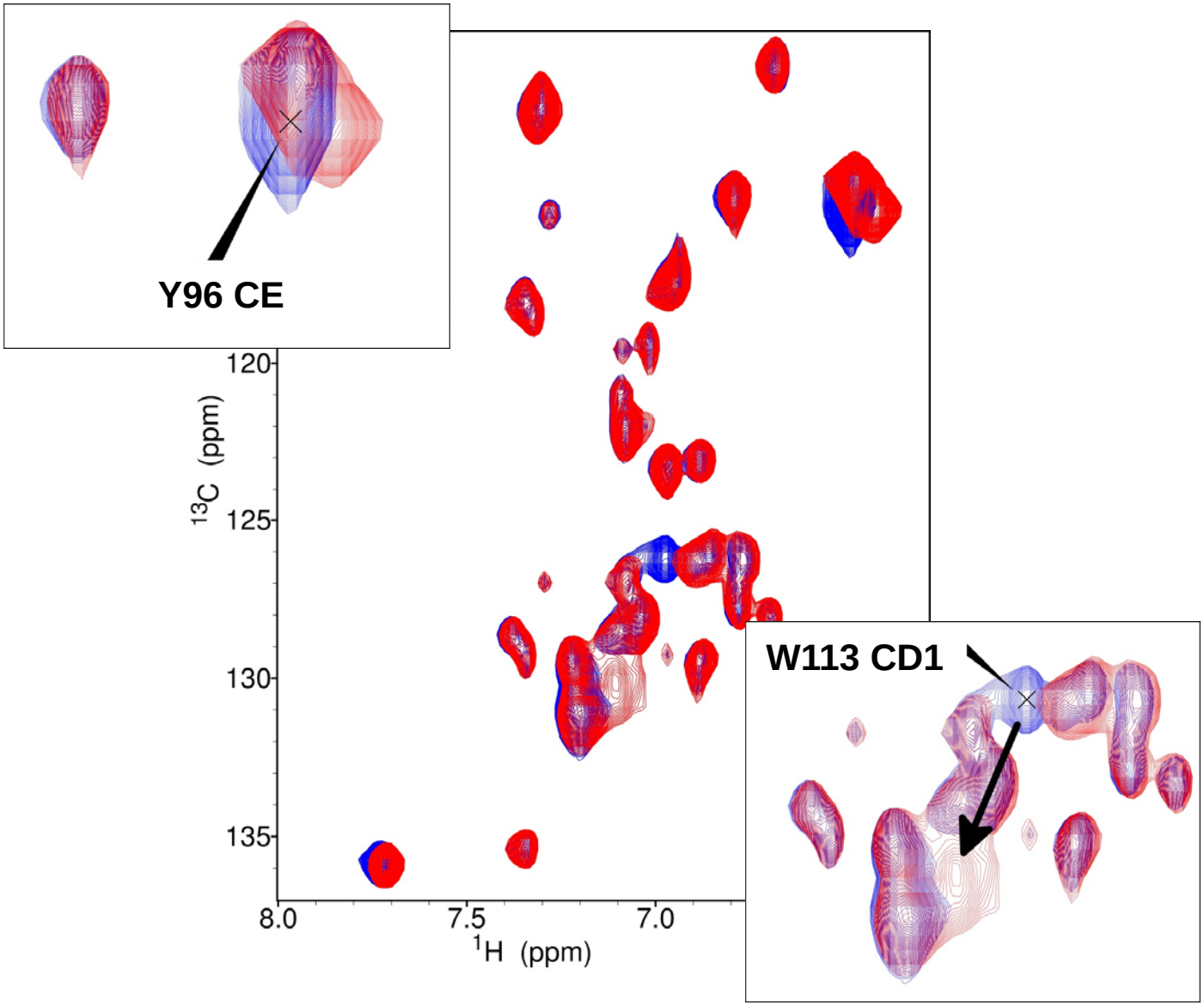

Fig. S3 B,C

B

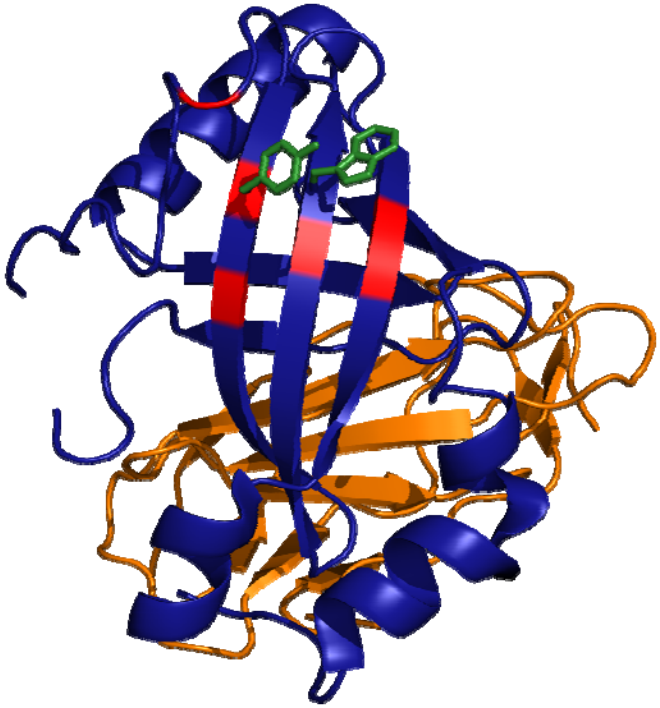

C

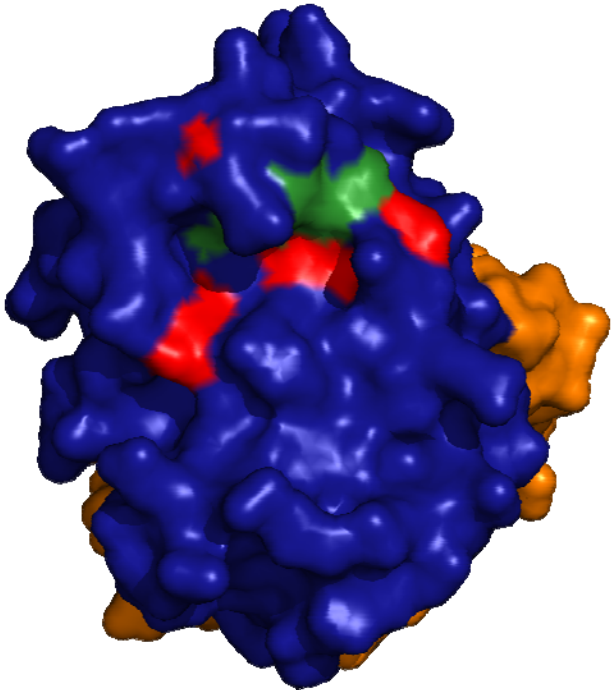

Fig. S3

NMR based localization of site of AI-4-57 binding on CBFβ.

A. Aromatic region of the ^{13}C-^{1}H HSQC spectrum of CBFβ alone (blue) and CBFβ + AI-4-57 (red) showing chemical shift changes for sidechain resonances of W113 and Y96, implicating them as being part of the binding site for AI-4-57. B. Ribbon representation of the structure of the Runt domain – CBFβ complex (CBFβ in blue; RUNX1 Runt domain in orange; PDB 1E50). Amino acids with NH chemical shift changes >0.03 ppm (calculated using the equation $\Delta(^{15}N + {}^{1}HN) = |\Delta\delta HN| + (|\Delta\delta N|/4.69)$ upon AI-4-57 binding are colored red (R90, Y96, K98, G112, M122, G123). The sidechains of W113 and Y96 are displayed and colored in green. C. Surface representation of the structure in the same orientation as in B and with the same coloring scheme as B showing the putative binding pocket for AI-4-57.

Fig. S4

4A.

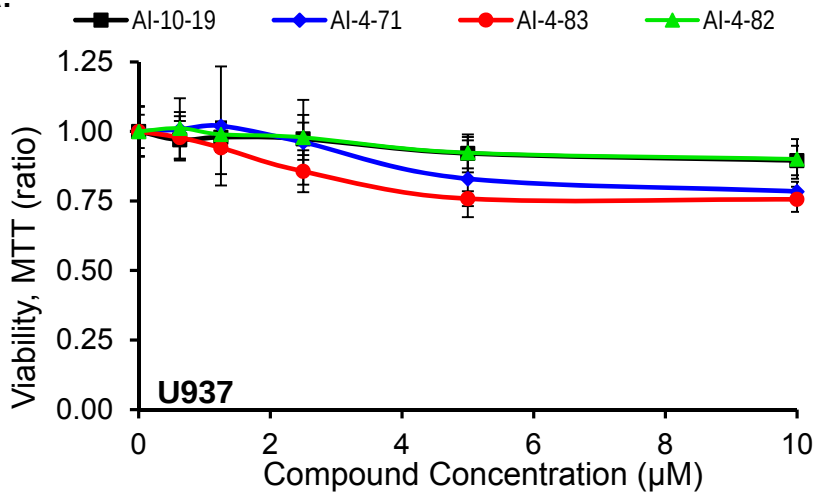
AI-10-19
AI-4-71
AI-4-83
AI-4-82
1.25
1.00
0.75
0.50
0.25
0.00
Viability, MTT (ratio)
U937
0
2
4
6
8
10
Compound Concentration (μM)

4B.

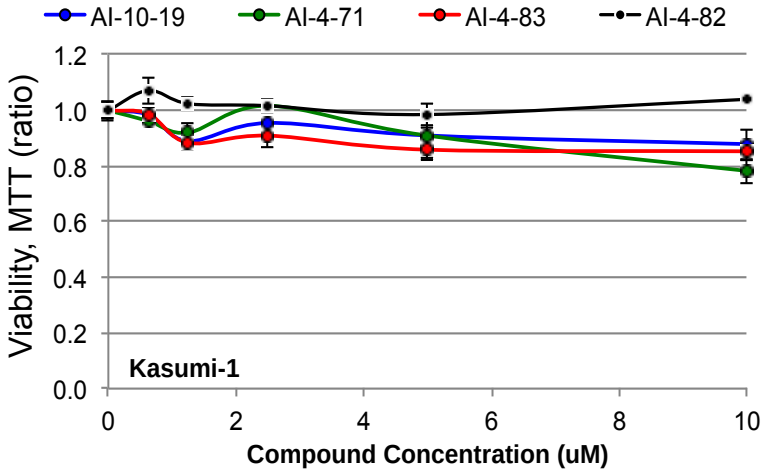
AI-10-19
AI-4-71
AI-4-83
AI-4-82
1.2
1.0
0.8
0.6
0.4
0.2
0.0
Viability, MTT (ratio)
Kasumi-1
0
2
4
6
8
10
Compound Concentration (uM)

Fig. S4

Inv(16) negative leukemic cell lines are not sensitive to bivalent compounds. Dose-dependent effect of 24 hour treatment of (A) U937 cells and (B) Kasumi-1 cells, with bivalent inhibitors with varying linker lengths measured by MTT assay; each symbol represents the mean of triplicate experiments; error bars represent the S.D.

Fig. S5

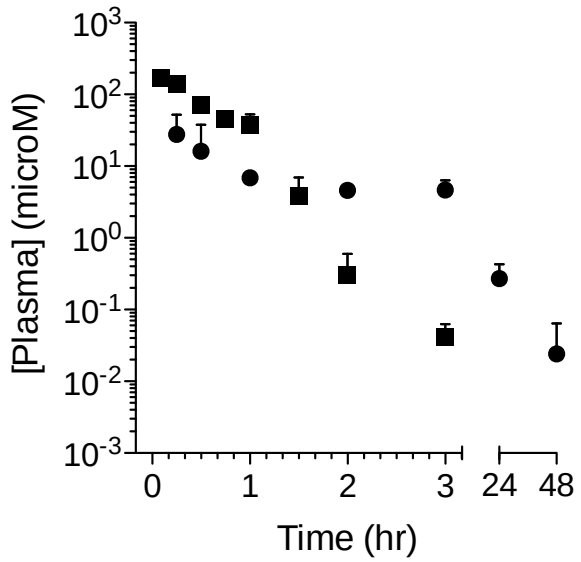

	AI-4-57	AI-10-49
Half-life (min)	36.6	379.9
$AUC_{0-\infty}$ (micromol•min/L)	5701.5	3752.9
Mean Residence Time (min)	27.7	373.2
Volume of Distribution (L)	0.7	1.1
Clearance (L/min)	0.013	0.002

Fig. S5

Plasma concentration data as a function of time for AI-4-57 (■) and AI-10-49 (●) and derived pharmacokinetic parameters for AI-4-57 and AI-10-49.

Fig. S6

6A.

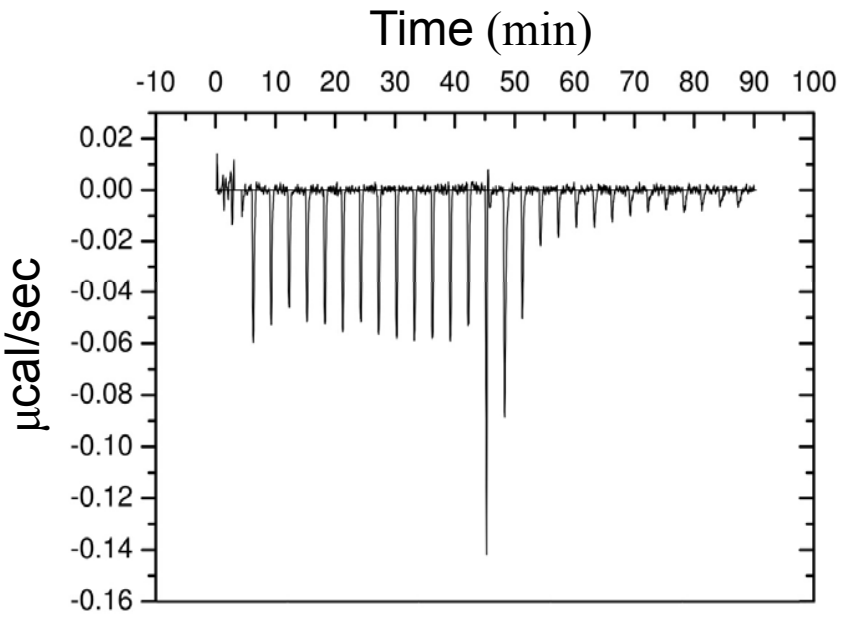

6B.

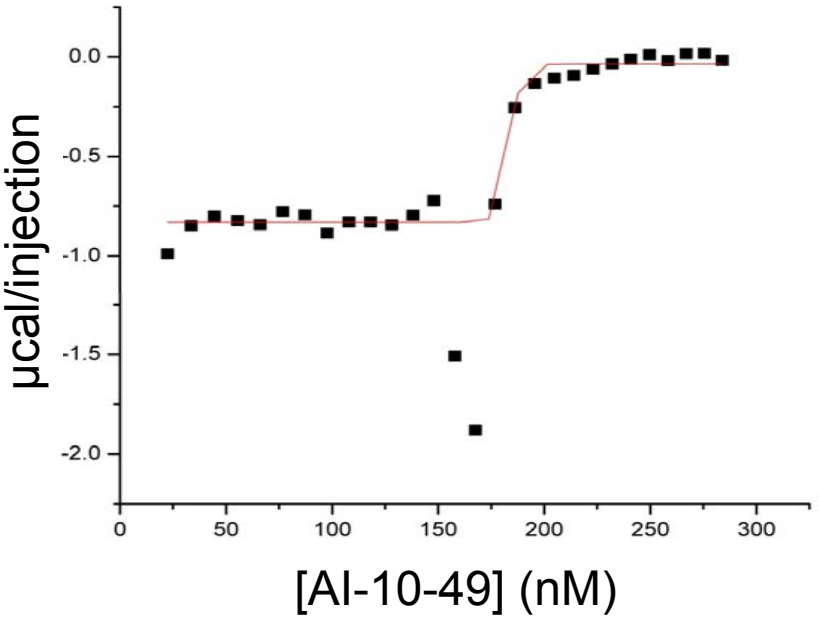

K_D = 168 ± 11 nM
N = 0.54 ± 0.03

Fig. S6

Isothermal titration calorimetry characterization of binding of AI-10-49 to CBFβ-SMMHC.

A. Results of one representative experiment for injection of 2 μM AI-10-49 into 400 nM CBFβ-SMMHC. B. Results of fitting the data to a one site model including derived dissociation constant (K_D) and stoichiometry (N) from 3 independent measurements ± S.D.

Fig. S7

A.

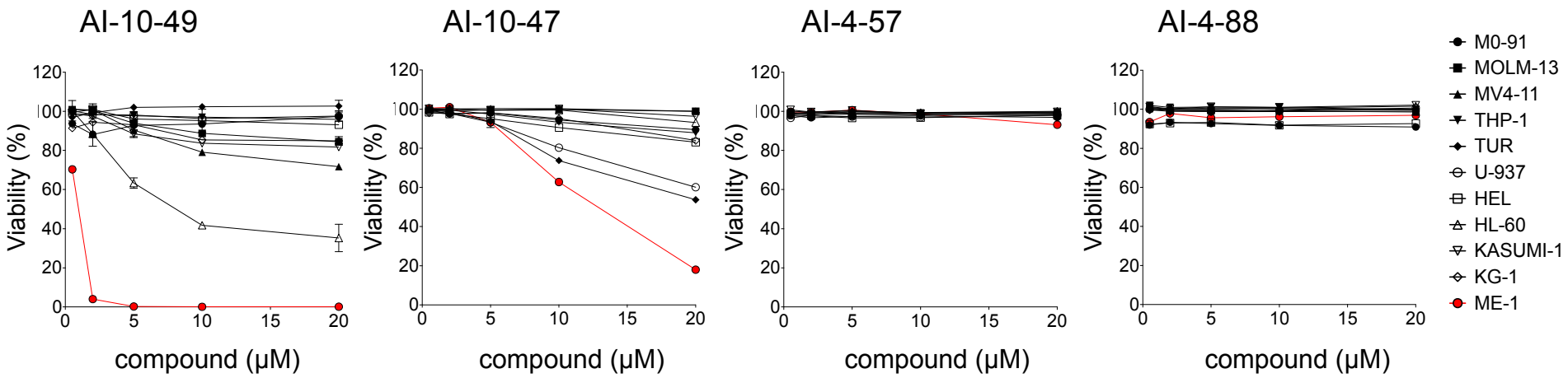

B.

Cell Line	Morphology	Type	Mutations	LD50 (μM) AI-10-49
MO-91	monoblastic	AML-M0	TEL-TRKC; const. active STAT	>20
MOLM-13	monocytic	AML-M5	MLL-AF9	>20
MV4-11	monocytic	AML-M5a	MLL-AF4, FLT3-ITD	>20
THP-1	monocytic	AML-M5	MLL-AF9	>20
TUR	monocytic	AML, M5	CALM-AF10; TPA-U937-Resis	>20
U937	monocytic	AML, M5	CALM-AF10	>20
HEL	erythroleukemia	AML-M6	JAK2V617F	>20
HL-60	promyelocytic	AML-M2	c-MYC amplification	4.5
KASUMI-1	myelomonocytic	AML-M2	AML1-ETO; c-KIT-N822K	>20
KG-1	promyelocyte	AML		>20
ME-1	myelomonocytic	AML-M4Eo	CBFβ-SMMHC	0.7

Fig. S7

AI-10-49 displays specific inhibition of inv(16)-positive cell line ME-1. A. Dose response viability of 11 AML cell lines at 24 hours treatment with AI-10-49, and monovalent compounds AI-10-47, AI-4-57 and AI-10-88. The sensitive inv(16)-positive ME-1 cell line is represented in red. Each symbol represents the average for an individual cell line from duplicate treatments at the indicated concentration. Five concentrations were tested for each compound (0.5, 2, 5, 10, 20 μM). Error bars represent the S.D. B. Disease classification and genetic information for the 11 AML cell lines and median lethal dose (LD_{50}) values for treatment with AI-10-49.

Fig. S8

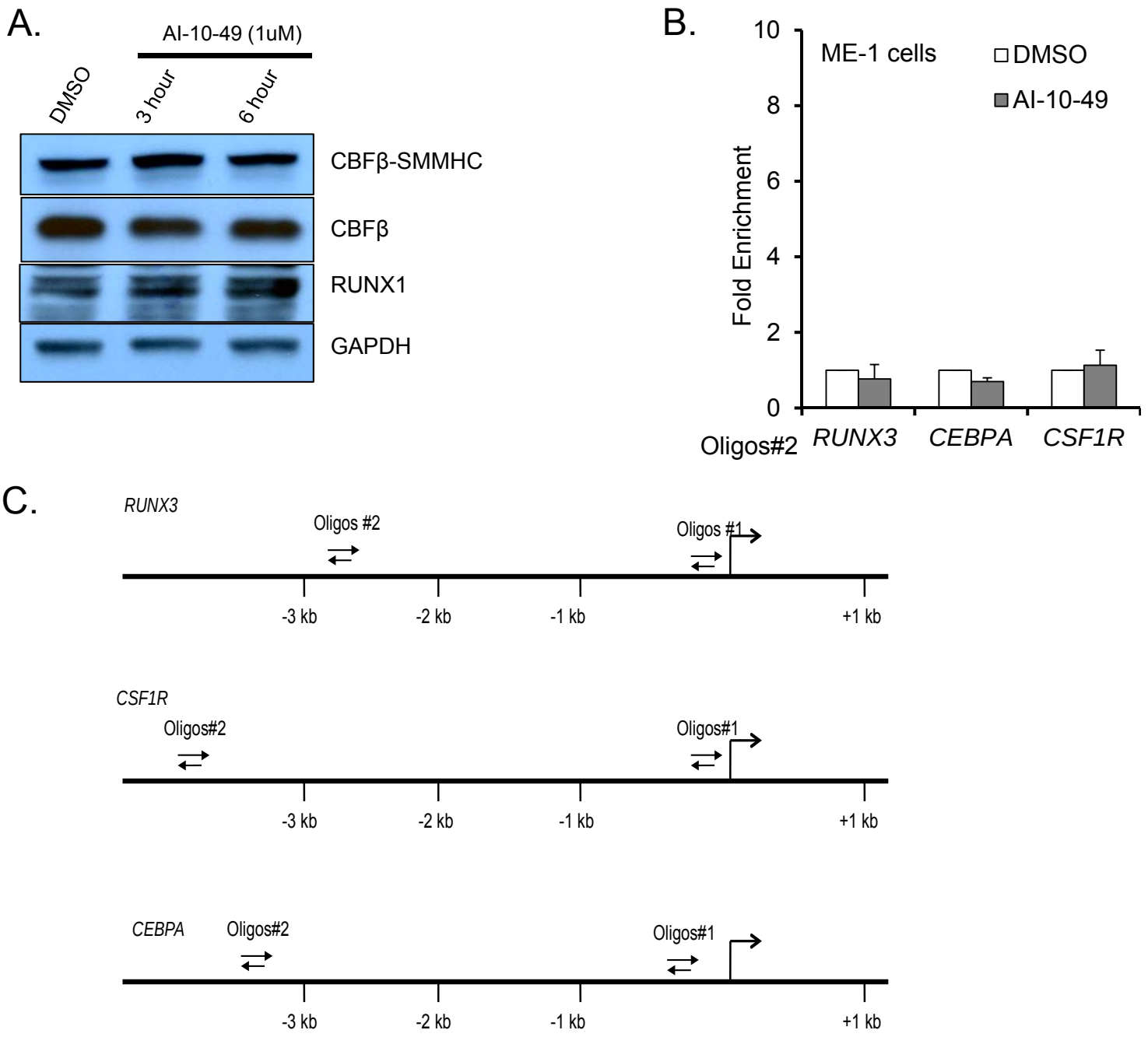
A.
AI-10-49 (1uM)
DMSO
3 hour
6 hour
CBFβ-SMMHC
CBFβ
RUNX1
GAPDH
B.
ME-1 cells
DMSO
AI-10-49
Fold Enrichment
10
8
6
4
2
0
Oligos#2
RUNX3
CEBPA
CSF1R
C.
RUNX3
Oligos #2
Oligos #1
-3 kb
-2 kb
-1 kb
+1 kb
CSF1R
Oligos#2
Oligos#1
-3 kb
-2 kb
-1 kb
+1 kb
CEBPA
Oligos#2
Oligos#1
-3 kb
-2 kb
-1 kb
+1 kb

Fig. S8

Effects of AI-10-49 on CBF stability and function in ME-1 cells (related to Figure 2). A. Immunoblot analysis of RUNX1, CBFβ, and CBFβ-SMMHC protein levels in whole cell lysates used for immunoprecipitation assay (Figure 2A); B. Chromatin immunoprecipitation analysis of RUNX1 occupancy at *RUNX3, CSF1R* and *CEBPA* loci using control oligo#2 sets in DNA from cells treated with DMSO or 1 μM AI-10-49 for 6 hours, and expressed as fold enrichment relative to DMSO; each symbol represents the mean of triplicate replicates; error bars represent the S.D. F. Schematic depicting the genomic position of Oligos#1 and control Oligo#2 primer sets, used for chromatin immunoprecipitation at the *RUNX3*, *CSF1R* and *CEBPA* loci.

Fig. S9

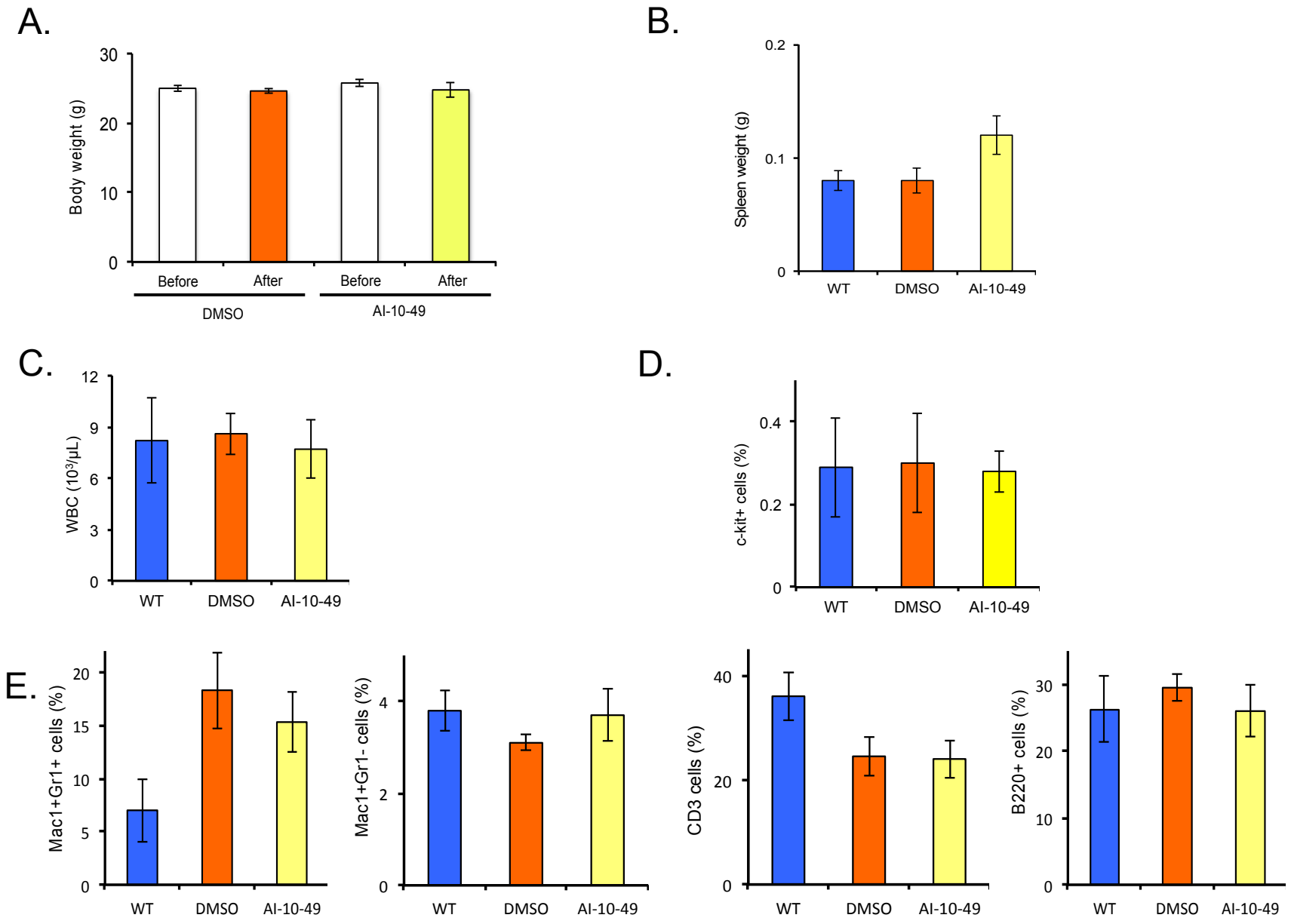
A.
Body weight (g)
30
20
10
0
Before
After
Before
After
DMSO
AI-10-49
B.
Spleen weight (g)
0.2
0.1
0
WT
DMSO
AI-10-49
C.
WBC (10³/μL)
12
9
6
3
0
WT
DMSO
AI-10-49
D.
c-kit+ cells (%)
0.4
0.2
0
WT
DMSO
AI-10-49
E.
Mac1+Gr1+ cells (%)
20
15
10
5
0
WT
DMSO
AI-10-49
Mac1+Gr1- cells (%)
4
2
0
WT
DMSO
AI-10-49
CD3 cells (%)
40
20
0
WT
DMSO
AI-10-49
B220+ cells (%)
30
20
10
0
WT
DMSO
AI-10-49

Fig. S9

Toxicology analysis of wild type mice treated with AI-10-49. Mice were not treated (Con, blue), or treated with a daily dose of DMSO (DMSO, orange) or 200 mg/kg/day AI-10-49 in DMSO (AI-10-49, yellow) for seven days. Mice were analyzed 1 day after last treatment dose. A. Body weight before and after treatment. B. Spleen weight before and after treatment. C. Cellularity of peripheral blood white blood cells. D. Percentage of immature [c-kit(+)] cells in peripheral blood. E. Percentage of granulocytes, monocytes, B cells, and T cells in peripheral blood. Each symbol represents the mean of values from three to four animals; error bars represent the S.D.

Fig. S10

A.

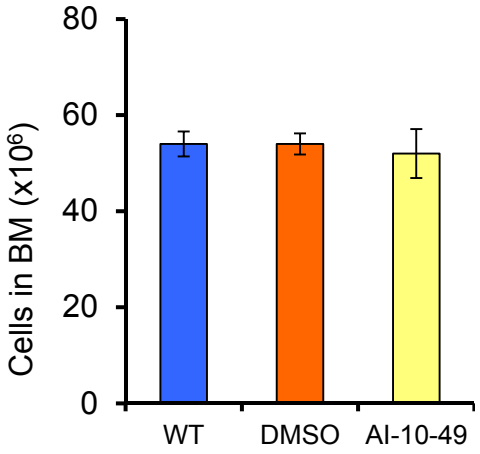
80
60
40
20
0
Cells in BM (x10^6)
WT
DMSO
AI-10-49

B.

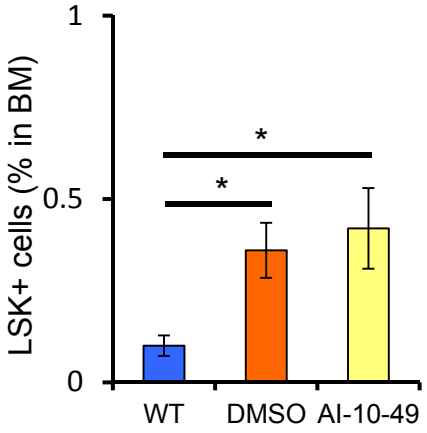
1
0.5
0
LSK+ cells (% in BM)
*
*
WT
DMSO
AI-10-49

C.

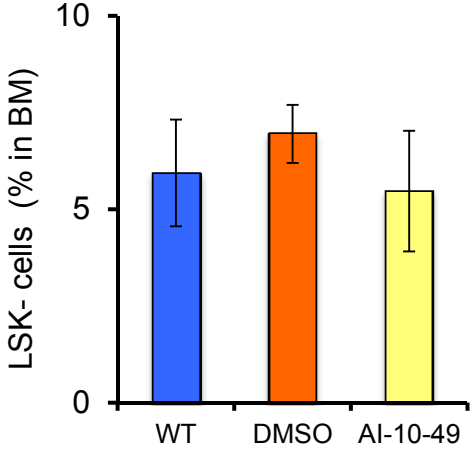
10
5
0
LSK- cells (% in BM)
WT
DMSO
AI-10-49

D.

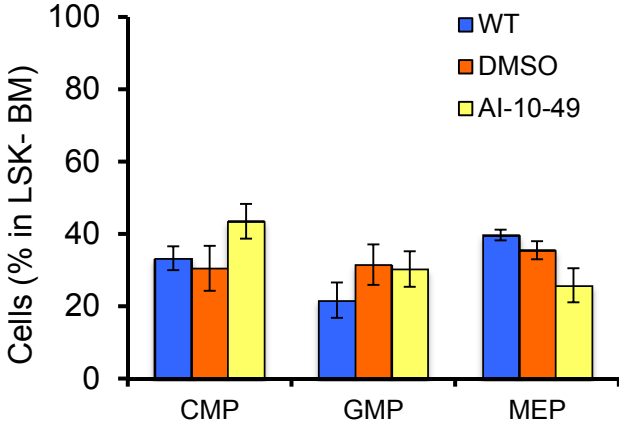
100
80
60
40
20
0
Cells (% in LSK- BM)
WT
DMSO
AI-10-49
CMP
GMP
MEP

Fig. S10

Toxicology analysis of bone marrow progenitors of wild type mice with no treatment, treatment with DMSO, or treatment with 200 mg/kg/day AI-10-49 in DMSO. A. Cellularity of bone marrow. B. Percentage of stem and early progenitor cells [LSK+: Lin(-)Sca1(+)ckit(+)] in bone marrow (BM). C. Percentage of early progenitor cells [LSK-: Lin(-)Sca1(-)ckit(+)] in BM; D. Percentage of each progenitor cell compartment, including common myeloid progenitors [CMP: LSK-,CD34(+)CD16/32(-)], megakaryocyte/erythroid progenitors [MEP: LSK-, CD34(-)CD16/32(-)], and granulocyte/monocyte progenitors [GMP: LSK-, CD34(+)CD16/32(+)], in LSK- BM cells. Each symbol represents the mean of values from three to four animals; error bars represent the S.D. Significance calculated as unpaired t-test, $P<0.05$ (*) or $P<0.001$(***).

Fig. S11

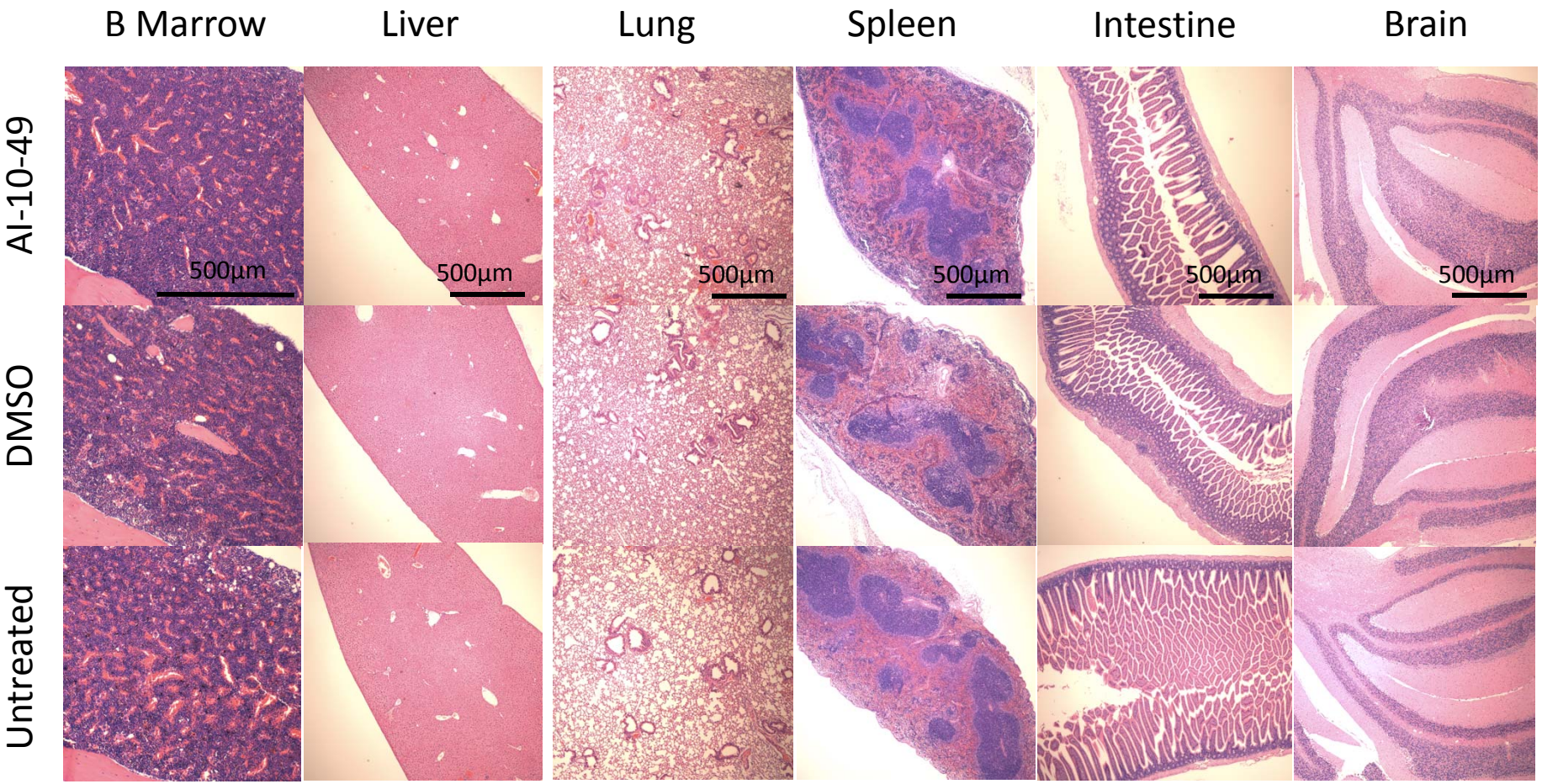
B Marrow
Liver
Lung
Spleen
Intestine
Brain
AI-10-49
DMSO
Untreated
500μm
500μm
500μm
500μm
500μm
500μm

Fig. S11

Toxicology analysis in tissues of mice treated with AI-10-49. Representative examples of Hematoxilyn & eosin staining of indicated tissues in mice treated for 7 days with 200 mg/kg/day AI-10-49 in DMSO (top), DMSO (middle), or untreated (bottom).

Fig. S12

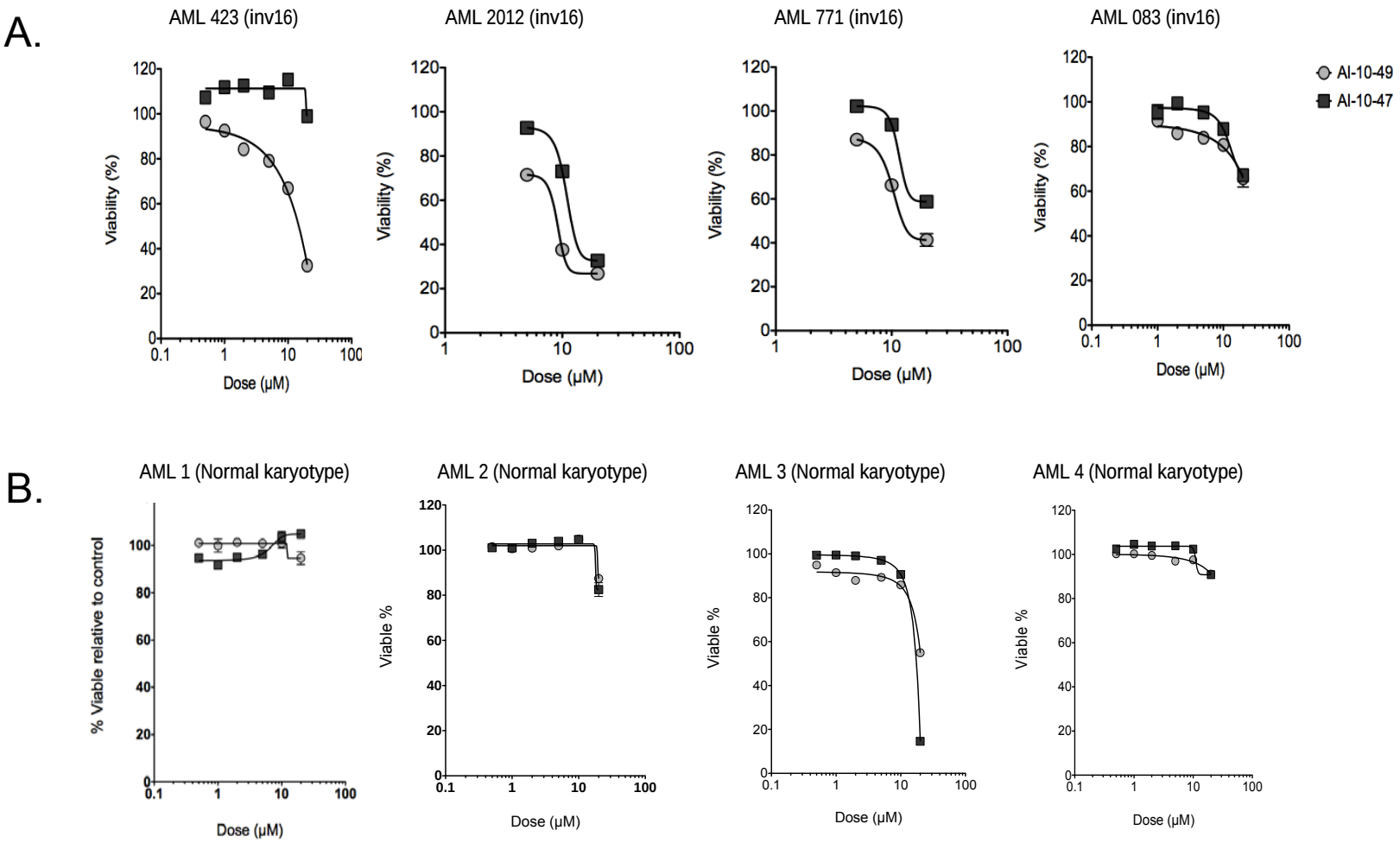
A.
AML 423 (inv16)
AML 2012 (inv16)
AML 771 (inv16)
AML 083 (inv16)
Viability (%)
Dose (μM)
AI-10-49
AI-10-47
B.
AML 1 (Normal karyotype)
AML 2 (Normal karyotype)
AML 3 (Normal karyotype)
AML 4 (Normal karyotype)
% Viable relative to control
Viable %
Dose (μM)

Fig. S12

Efficacy of AI-10-47 and AI-10-49 on human AML primary blasts. A. Dose response analysis of purified CD34(+) primary human inv(16) AML samples after 48 hour treatment with AI-10-47 or AI-10-49; B. Dose response analysis of purified CD34(+) primary human AML samples with normal karyotype. Viability was determined using Annexin V and 7AAD by flow cytometry and represented as percent of DMSO control. Limitations in the available number of purified CD34(+) primary cells for AML2012, AML 771 and AML083 made it necessary to evaluate a reduced number of data points for these samples. Each symbol represents the average for an individual sample from duplicate or triplicate treatments. Error bars represent the S.D.

Fig. S13 A,B

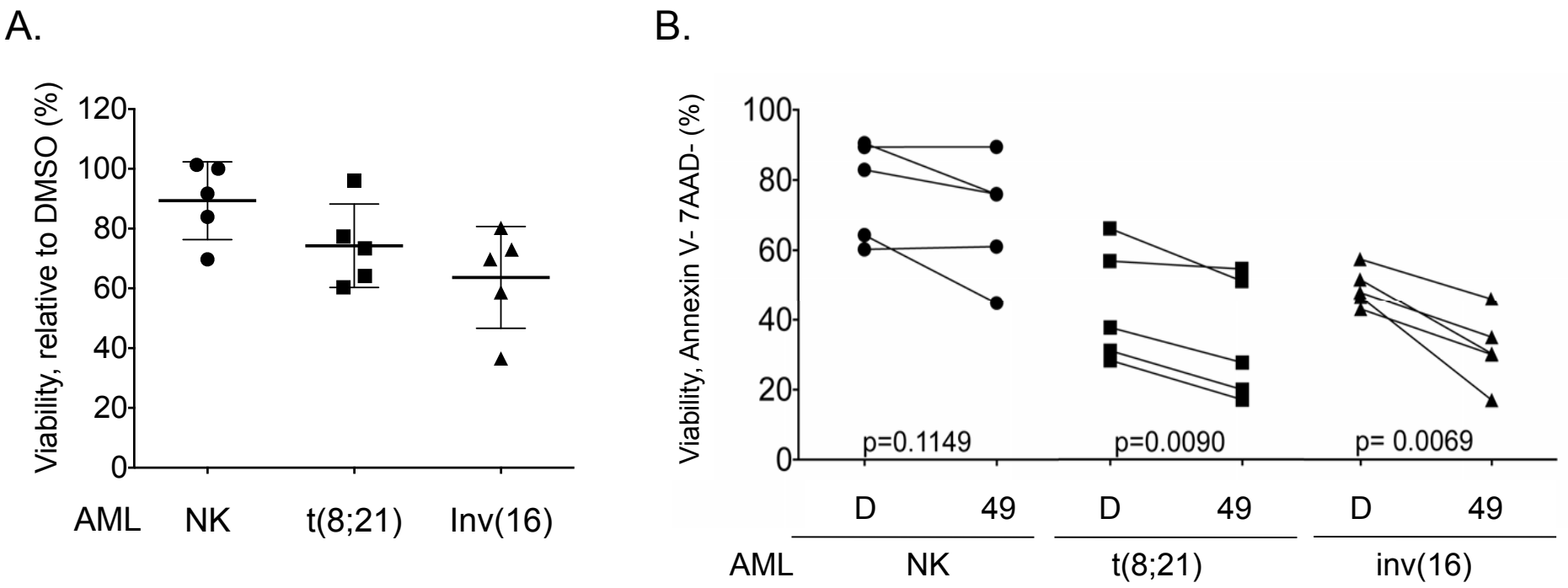
A.
Viability, relative to DMSO (%)
120
100
80
60
40
20
0
AML
NK
t(8;21)
Inv(16)
B.
Viability, Annexin V- 7AAD- (%)
100
80
60
40
20
0
p=0.1149
p=0.0090
p= 0.0069
D
49
D
49
D
49
AML
NK
t(8;21)
inv(16)

Fig. S13 C

C.

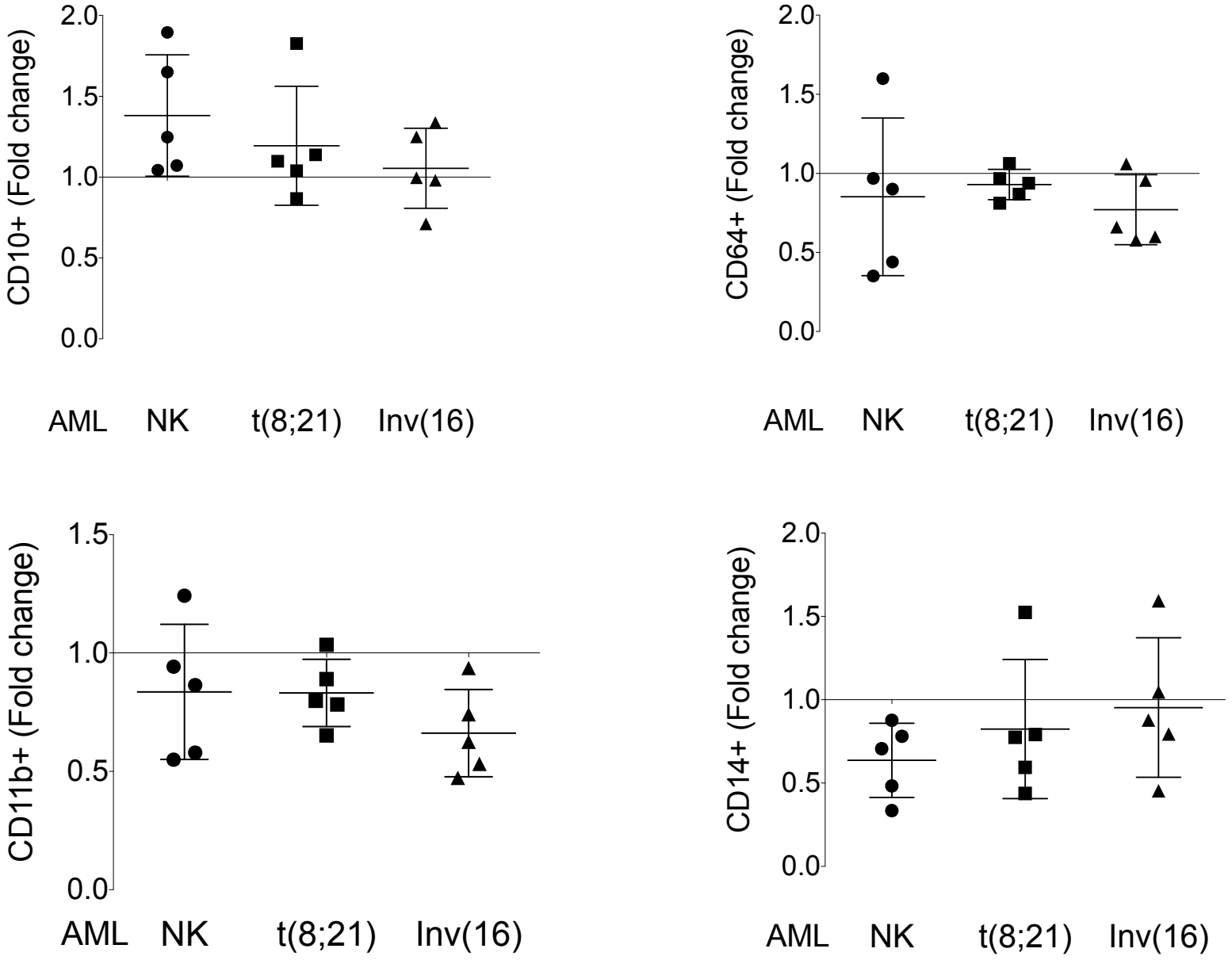
CD10+ (Fold change)
2.0
1.5
1.0
0.5
0.0
AML
NK
t(8;21)
Inv(16)
CD64+ (Fold change)
2.0
1.5
1.0
0.5
0.0
AML
NK
t(8;21)
Inv(16)
CD11b+ (Fold change)
1.5
1.0
0.5
0.0
AML
NK
t(8;21)
Inv(16)
CD14+ (Fold change)
2.0
1.5
1.0
0.5
0.0
AML
NK
t(8;21)
Inv(16)

Fig. S13

AI-10-49 reduces the viability but does not induce differentiation of inv(16) AML cells. Sorted CD34+ cells from patient AML (n=5 per group) with normal karyotype (NK), chromosome translocation t(8;21), or chromosome inversion inv(16) were treated for 48 hours with DMSO or 10 μM AI-10-49. A. Percent viability (Annexin V-, 7AAD-) of AI-10-49 treated cells relative to control (DMSO). Each symbol represents the average for an individual sample from duplicate treatments. The line represents the mean. Error bars represent the S.D. The partial reduction in the viability of t(8;21) human AML cells obtained could result from a poly-valent interaction of AI-10-49 with CBFβ bound to AML1-ETO, which is also an oligomeric fusion protein. B. Same as A shown as percentage of viable cells (Annexin V-/7AAD-). Each symbol represents the average for an individual sample from duplicate treatments. The line represents the mean. Error bars represent the S.D. Significance calculated as a two-tailed paired t-test. C. Fold change in expression of CD10, CD64, CD11b, or CD14 in viable cells after treatment with 10 μM AI-10-49. Each symbol represents the average for an individual sample from duplicate treatments. The line represents the mean. Error bars represent the S.D. Fold change is represented relative to DMSO control. Each symbol represents the average of a primary AML sample.

REFERENCES

1. C. C. Kumar, Genetic abnormalities and challenges in the treatment of acute myeloid leukemia. *Genes Cancer* **2**, 95–107 (2011). Medline doi:10.1177/1947601911408076

2. P. Liu, S. A. Tarlé, A. Hajra, D. F. Claxton, P. Marlton, M. Freedman, M. J. Siciliano, F. S. Collins, Fusion between transcription factor CBF beta/PEBP2 beta and a myosin heavy chain in acute myeloid leukemia. *Science* **261**, 1041–1044 (1993). Medline doi:10.1126/science.8351518

3. L. H. Castilla, L. Garrett, N. Adya, D. Orlic, A. Dutra, S. Anderson, J. Owens, M. Eckhaus, D. Bodine, P. P. Liu, The fusion gene Cbfb-MYH11 blocks myeloid differentiation and predisposes mice to acute myelomonocytic leukaemia. *Nat. Genet.* **23**, 144–146 (1999). Medline doi:10.1038/13776

4. L. H. Castilla, P. Perrat, N. J. Martinez, S. F. Landrette, R. Keys, S. Oikemus, J. Flanegan, S. Heilman, L. Garrett, A. Dutra, S. Anderson, G. A. Pihan, L. Wolff, P. P. Liu, Identification of genes that synergize with Cbfb-MYH11 in the pathogenesis of acute myeloid leukemia. *Proc. Natl. Acad. Sci. U.S.A.* **101**, 4924–4929 (2004). Medline doi:10.1073/pnas.0400930101

5. F. Ravandi, A. K. Burnett, E. D. Agura, H. M. Kantarjian, Progress in the treatment of acute myeloid leukemia. *Cancer* **110**, 1900–1910 (2007). Medline doi:10.1002/cncr.23000

6. N. Adya, L. H. Castilla, P. P. Liu, Function of CBFbeta/Bro proteins. *Semin. Cell Dev. Biol.* **11**, 361–368 (2000). Medline doi:10.1006/scdb.2000.0189

7. M. F. de Bruijn, N. A. Speck, Core-binding factors in hematopoiesis and immune function. *Oncogene* **23**, 4238–4248 (2004). Medline doi:10.1038/sj.onc.1207763

8. S. M. Lukasik, L. Zhang, T. Corpora, S. Tomanicek, Y. Li, M. Kundu, K. Hartman, P. P. Liu, T. M. Laue, R. L. Biltonen, N. A. Speck, J. H. Bushweller, Altered affinity of CBF beta-SMMHC for Runx1 explains its role in leukemogenesis. *Nat. Struct. Biol.* **9**, 674–679 (2002). Medline doi:10.1038/nsb831

9. Y. H. Kuo, S. F. Landrette, S. A. Heilman, P. N. Perrat, L. Garrett, P. P. Liu, M. M. Le Beau, S. C. Kogan, L. H. Castilla, Cbf beta-SMMHC induces distinct abnormal myeloid progenitors able to develop acute myeloid leukemia. *Cancer Cell* **9**, 57–68 (2006). Medline doi:10.1016/j.ccr.2005.12.014

10. P. D. Kottaridis, R. E. Gale, S. E. Langabeer, M. E. Frew, D. T. Bowen, D. C. Linch, Studies of *FLT3* mutations in paired presentation and relapse samples from patients with acute myeloid leukemia: Implications for the role of *FLT3* mutations in leukemogenesis, minimal residual disease detection, and possible therapy with FLT3 inhibitors. *Blood* **100**, 2393–2398 (2002). Medline doi:10.1182/blood-2002-02-0420

11. L. Y. Shih, D. C. Liang, C. F. Huang, Y. T. Chang, C. L. Lai, T. H. Lin, C. P. Yang, I. J. Hung, H. C. Liu, T. H. Jaing, L. Y. Wang, T. C. Yeh, Cooperating mutations of receptor tyrosine kinases and *Ras* genes in childhood core-binding factor acute myeloid leukemia and a comparative analysis on paired diagnosis and relapse samples. *Leukemia* **22**, 303–307 (2008). Medline doi:10.1038/sj.leu.2404995

12. Y. Nakano, H. Kiyoi, S. Miyawaki, N. Asou, R. Ohno, H. Saito, T. Naoe, Molecular evolution of acute myeloid leukaemia in relapse: Unstable N-*ras* and *FLT3* genes compared with *p53* gene. *Br. J. Haematol.* **104**, 659–664 (1999). Medline doi:10.1046/j.1365-2141.1999.01256.x

13. M. J. Gorczynski, J. Grembecka, Y. Zhou, Y. Kong, L. Roudaia, M. G. Douvas, M. Newman, I. Bielnicka, G. Baber, T. Corpora, J. Shi, M. Sridharan, R. Lilien, B. R. Donald, N. A. Speck, M. L. Brown, J. H. Bushweller, Allosteric inhibition of the protein-protein interaction between the leukemia-associated proteins Runx1 and CBFbeta. *Chem. Biol.* **14**, 1186–1197 (2007). Medline doi:10.1016/j.chembiol.2007.09.006

14. S. A. Heilman, Y. H. Kuo, C. S. Goudswaard, P. J. Valk, L. H. Castilla, Cbfbeta reduces Cbfbeta-SMMHC–associated acute myeloid leukemia in mice. *Cancer Res.* **66**, 11214–11218 (2006). Medline doi:10.1158/0008-5472.CAN-06-0959

15. X. Huang, J. W. Peng, N. A. Speck, J. H. Bushweller, Solution structure of core binding factor beta and map of the CBF alpha binding site. *Nat. Struct. Biol.* **6**, 624–627 (1999). Medline doi:10.1038/10670

16. M. Mammen, S. K. Choi, G. M. Whitesides, Polyvalent interactions in biological systems: Implications for design and use of multivalent ligands and inhibitors. *Angew. Chem. Int. Ed.* **37**, 2754–2794 (1998). http://onlinelibrary.wiley.com/doi/10.1002/%28SICI%291521-3773%2819981102%2937:20%3C2754::AID-ANIE2754%3E3.0.CO;2-3/abstract

17. L. L. Kiessling, J. E. Gestwicki, L. E. Strong, Synthetic multivalent ligands as probes of signal transduction. *Angew. Chem. Int. Ed. Engl.* **45**, 2348–2368 (2006). Medline doi:10.1002/anie.200502794

18. F. R. Leroux, B. Manteau, J. P. Vors, S. Pazenok, Trifluoromethyl ethers—synthesis and properties of an unusual substituent. *Beilstein J. Org. Chem.* **4**, 13 (2008). Medline doi:10.3762/bjoc.4.13

19. B. Manteau, S. Pazenok, J. P. Vors, F. R. Leroux, New trends in the chemistry of alpha-fluorinated ethers, thioethers, amines and phosphines. *J. Fluor. Chem.* **131**, 140–158 (2010). doi:10.1016/j.jfluchem.2009.09.009

20. C. K. Cheng, L. Li, S. H. Cheng, K. M. Lau, N. P. Chan, R. S. Wong, M. M. Shing, C. K. Li, M. H. Ng, Transcriptional repression of the *RUNX3/AML2* gene by the t(8;21) and inv(16) fusion proteins in acute myeloid leukemia. *Blood* **112**, 3391–3402 (2008). Medline doi:10.1182/blood-2008-02-137083

21. H. Guo, O. Ma, N. A. Speck, A. D. Friedman, Runx1 deletion or dominant inhibition reduces *Cebpa* transcription via conserved promoter and distal enhancer sites to favor monopoiesis over granulopoiesis. *Blood* **119**, 4408–4418 (2012). Medline doi:10.1182/blood-2011-12-397091

22. D. E. Zhang, K. Fujioka, C. J. Hetherington, L. H. Shapiro, H. M. Chen, A. T. Look, D. G. Tenen, Identification of a region which directs the monocytic activity of the colony-stimulating factor 1 (macrophage colony-stimulating factor) receptor promoter and binds PEBP2/CBF (AML1). *Mol. Cell. Biol.* **14**, 8085–8095 (1994). Medline

23. W. Cao, M. Britos-Bray, D. F. Claxton, C. A. Kelley, N. A. Speck, P. P. Liu, A. D. Friedman, CBFbeta-SMMHC, expressed in M4Eo AML, reduced CBF DNA-binding and inhibited the G1 to S cell cycle transition at the restriction point in myeloid and lymphoid cells. *Oncogene* **15**, 1315–1327 (1997). Medline doi:10.1038/sj.onc.1201305

24. J. Markus, M. T. Garin, J. Bies, N. Galili, A. Raza, M. J. Thirman, M. M. Le Beau, J. D. Rowley, P. P. Liu, L. Wolff, Methylation-independent silencing of the tumor suppressor INK4b (p15) by CBFbeta-SMMHC in acute myelogenous leukemia with inv(16). *Cancer Res.* **67**, 992–1000 (2007). Medline doi:10.1158/0008-5472.CAN-06-2964

25. C. Haferlach, F. Dicker, A. Kohlmann, S. Schindela, T. Weiss, W. Kern, S. Schnittger, T. Haferlach, AML with CBFB-MYH11 rearrangement demonstrate RAS pathway alterations in 92% of all cases including a high frequency of NF1 deletions. *Leukemia* **24**, 1065–1069 (2010). Medline doi:10.1038/leu.2010.22

26. L. Xue, J. A. Pulikkan, P. J. Valk, L. H. Castilla, NrasG12D oncoprotein inhibits apoptosis of preleukemic cells expressing Cbfβ-SMMHC via activation of MEK/ERK axis. *Blood* **124**, 426–436 (2014). Medline doi:10.1182/blood-2013-12-541730

27. A. T. Look, Oncogenic transcription factors in the human acute leukemias. *Science* **278**, 1059–1064 (1997). Medline doi:10.1126/science.278.5340.1059

28. M. Ladanyi, The emerging molecular genetics of sarcoma translocations. *Diagn. Mol. Pathol.* **4**, 162–173 (1995). Medline doi:10.1097/00019606-199509000-00003

29. D. Hessels, J. A. Schalken, Recurrent gene fusions in prostate cancer: Their clinical implications and uses. *Curr. Urol. Rep.* **14**, 214–222 (2013). Medline doi:10.1007/s11934-013-0321-1

30. S. V. Frye, The art of the chemical probe. *Nat. Chem. Biol.* **6**, 159–161 (2010). Medline doi:10.1038/nchembio.296

31. K. Bahrami, M. M. Khodaei, A. Nejati, Synthesis of 1,2-disubstituted benzimidazoles, 2-substituted benzimidazoles and 2-substituted benzothiazoles in SDS micelles. *Green Chem.* **12**, 1237 (2010). doi:10.1039/c000047g

32. Q. Wang, T. Stacy, J. D. Miller, A. F. Lewis, T. L. Gu, X. Huang, J. H. Bushweller, J. C. Bories, F. W. Alt, G. Ryan, P. P. Liu, A. Wynshaw-Boris, M. Binder, M. Marín-Padilla, A. H. Sharpe, N. A. Speck, The CBFbeta subunit is essential for CBFalpha2 (AML1) function in vivo. *Cell* **87**, 697–708 (1996). Medline doi:10.1016/S0092-8674(00)81389-6

33. R. Ihaka, R. Gentleman, R: A language for data analysis and graphics. *J. Comput. Graph. Stat.* **5**, 299 (1996).

34. M. L. Guzman, C. F. Swiderski, D. S. Howard, B. A. Grimes, R. M. Rossi, S. J. Szilvassy, C. T. Jordan, Preferential induction of apoptosis for primary human leukemic stem cells. *Proc. Natl. Acad. Sci. U.S.A.* **99**, 16220–16225 (2002). Medline doi:10.1073/pnas.252462599

35. M. L. Guzman, R. M. Rossi, L. Karnischky, X. Li, D. R. Peterson, D. S. Howard, C. T. Jordan, The sesquiterpene lactone parthenolide induces apoptosis of human acute myelogenous leukemia stem and progenitor cells. *Blood* **105**, 4163–4169 (2005). Medline doi:10.1182/blood-2004-10-4135